The multi-ion nature of the cGMP-gated channel from vertebrate rods

Federico Sesti*, Elisabeth Eismann†, U. Benjamin Kaupp†, Mario Nizzari* and Vincent Torre‡§

†*Institut für Biologische Informationsverarbeitung, Forschungszentrum, Julich, Germany,* **Consorzio INFM and* ‡*Dipartimento di Fisica, Università di Genova, Via Dodecaneso 33, 16146 Genova, Italy*

1. Native cGMP-gated channels were studied in rod outer segments of the larval tiger salamander, *Ambystoma tigrinum*. The α-subunit of the cGMP-gated channel, here referred to as the wild type (WT), and mutant channels were heterologously expressed in *Xenopus laevis* oocytes. These channels were studied in excised membrane patches in the inside-out configuration and were activated by the addition of 100 or 500 μM cGMP. The current carried by monovalent cations was measured under voltage-clamp conditions.

2. In the presence of 110 mM Na^+ in the extracellular medium and different amounts of Na^+ in the intracellular medium, the I–V relations of the native channel could be described by a single-site model with a profile of Gibbs free energy with two barriers and a well. A similar result was obtained in the presence of 110 mM Li^+ in the extracellular medium and different amounts of Li^+ in the intracellular medium. The well depth was $1{\cdot}4RT$ (where R is the gas constant and T is the absolute temperature) for both Li^+ and Na^+.

3. The I–V relations of the native channel in the presence of 110 mM Na^+ on one side of the membrane and 110 mM Li^+ on the other side could not be described by the same single-site model with identical values of barriers and well obtained in the presence of Li^+ or Na^+ alone: the well for Li^+ had to be at least $4RT$.

4. In the presence of mixtures of 110 mM Li^+ and Cs^+ on the cytoplasmic side of the membrane, an anomalous mole fraction effect was observed both in the native and the WT channel. No anomalous behaviour was seen in the presence of Li^+–Na^+ and Li^+–NH_4^+ mixtures.

5. The anomalous mole fraction effect with mixtures of Li^+ and Cs^+ was not observed in the channel where glutamate 363 was mutated to a glutamine (E363Q) or an asparagine (E363N). When glutamate 363 was mutated to an aspartate (E363D), the anomalous mole fraction effect with mixtures of Li^+ and Cs^+ was still observed, although significantly reduced.

6. When lysine 346, arginine 369, aspartate 370 and glutamate 372 were neutralized by mutation to glutamine, the ion permeation through the mutant channels and the WT channel had largely similar properties.

7. The results here reported indicate that: (i) the native and the WT cGMP-gated channels are both multi-ion pores; (ii) the mutant channels E363Q and E363N behave as a single-ion pore; (iii) the multi-ion nature of the WT channel is primarily controlled by glutamate 363 and not by other charged residues in the pore region.

The ion channel controlled by light in vertebrate rod photoreceptor cells, usually referred to as the cGMP-gated channel, does not appreciably discriminate between monovalent alkali cations (Menini, 1990; Furman & Tanaka, 1990; Lühring, Hanke, Simmoteit & Kaupp, 1990) and is permeable to a variety of divalent cations (Colamartino, Menini & Torre, 1991). This channel is composed of at least two distinct but genetically related

§ To whom correspondence should be addressed.

subunits, designated as the α-subunit and the β-subunit. Upon heterologous expression in *Xenopus* oocytes, only the α-subunit constitutes a functional cGMP-gated channel, with properties similar to those of the native channel (Kaupp *et al.* 1989; Nizzari, Sesti, Giraudo, Virginio, Cattaneo & Torre, 1993). However, the fast-flickering behaviour and the blockage by L-*cis*-diltiazem characteristic of the native channel are observed only upon co-expression of α- and β-subunits (Chen, Peng, Dhallan, Ahamed, Reed & Yau, 1993). Whether the β-subunit contributes to the lining of the ion conducting pathway is not known.

Comparison with the protein sequences of K^+ channels has suggested that the pore region of the cGMP-gated channel is located between transmembrane segments H4 and H5 (Guy, Durell, Warmke, Drysdale & Ganetzky, 1991; Heginbotham, Abramson & MacKinnon, 1992; Bönigk *et al.* 1993; Goulding, Tibbs, Liu & Siegelbaum, 1993). Accordingly, a glutamate residue in position 363 of the α-subunit resides in the pore lumen of the cGMP-gated channel. When glutamate 363 is replaced by a glutamine, the mutant channel E363Q displays a different I–V relation and sensitivity to external divalent cations (Root & MacKinnon, 1993; Eismann, Müller, Heinemann & Kaupp, 1994).

An important issue for the understanding of the molecular basis of ionic permeation through cGMP-gated channels is to establish whether the channel behaves as a simple single-ion pore or whether it can be simultaneously occupied by more than one permeating ion, that is, whether it behaves as a multi-ion pore. Early studies of permeation through the cGMP-gated channel (Menini, Rispoli & Torre, 1988; Menini, 1990) described a simple saturation of the current when the concentration of the permeating ion was increased, in agreement with a simple single-ion behaviour. Furman & Tanaka (1990) reported some asymmetries of the reversal potential in the presence of bi-ionic solutions of NH_4^+–Na^+ and Cs^+–Na^+, suggesting that the channel could be a multi-ion channel. Possible deviations from the single-ion channel were reported by Rispoli & Detwiler (1990), describing an anomalous mole fraction effect in detached rods in the presence of Ca^{2+}, but this effect was observed only in the presence of nucleoside triphosphate. However, no anomalous mole fraction effect was observed in excised patches in the presence of mixtures of Na^+ and Li^+ (Menini, 1990) or Na^+ and Ca^{2+} (Zimmerman & Baylor, 1992). In addition, the success of a single-site model to account for the shape of the I–V relations in the presence of different amounts of Na^+, Ca^{2+} and Mg^{2+} has led to the notion that a single binding site dominates the ionic permeation through the cGMP-gated channel (Zimmerman & Baylor, 1992; Torre & Menini, 1994; Miller, Picones & Korenbrot, 1994).

The first aim of this paper is to provide definitive evidence that the native cGMP-gated channel is a multi-ion channel. Firstly, an anomalous mole fraction effect can be observed in the presence of mixtures of Li^+ and Cs^+, providing supporting evidence for the multi-ion nature of the native cGMP-gated channel. Secondly, an analysis of the permeation of Li^+ reveals that when the ionic activity of Li^+ in the bathing medium is increased from 5 to 50 mM, the channel decreases its affinity for Li^+. This transition between a high-affinity and a low-affinity binding site is reminiscent of Ca^{2+} channels (Hess & Tsien, 1984; Almers & McCleskey, 1984; Kuo & Hess, 1993*a*, *b*) and suggests that the ionic permeation of small alkali cations such as Li^+ or Na^+, under normal conditions, requires the simultaneous presence of at least two ions within the channel.

The second aim of this paper is to analyse the molecular basis of the multi-ion nature of the cGMP-activated channel. It will be shown that the α-subunit of the cGMP-activated channel (Kaupp *et al.* 1989) – here designated as the WT channel – is, like the native channel, a multi-ion channel. The multi-ion nature of the WT channel is specifically caused by the negative residue of glutamate 363 and not by other charged residues in the putative pore region. These results establish a novel and important analogy between cGMP-activated channels and Ca^{2+} channels (Kim, Morii, Sun, Imoto & Mori, 1993; Yang, Ellinor, Sather, Zhang & Tsien, 1993): in both channels the co-ordination of several glutamates provides the basis for multi-ion occupancy within the channel and subserves the transition between a high-affinity and a low-affinity binding site, necessary for a high ion turnover.

METHODS

Dissection and recording apparatus

Larval tiger salamanders, *Ambystoma tigrinum*, were decapitated and pithed. Mature *Xenopus laevis* were anaesthetized with 0·2% tricaine methanesulphonate (Sigma) and ovarian lobes were surgically removed. The preparation of isolated outer segments of tiger salamander rods was the same as that described in Sesti, Straforini, Lamb & Torre (1994). Oocytes from *Xenopus laevis* were prepared as described in Nizzari *et al.* 1993.

Experiments were performed on rod outer segments mechanically isolated from the retina of the larval *Ambystoma tigrinum* and on *Xenopus laevis* oocytes previously injected with WT or mutant channel mRNA. Currents activated by cGMP were recorded under voltage-clamp conditions from membrane patches in the inside-out configuration (Hamill, Marty, Neher, Sakmann & Sigworth, 1981), excised either from rod outer segments or injected *Xenopus* oocytes. The recording apparatus was the same as that described in Sesti *et al.* 1994.

Site-directed mutagenesis, *in vitro* transcription and functional expression

As shown in Fig. 1*A*, the amino acid sequence of the putative pore region of the WT cGMP-gated channel from bovine rods (Kaupp *et al.* 1989) contains five charged residues between lysine 346 and glutamate 372, indicated by arrows. Point mutations K346Q, E363Q, E363D, E363N, R369Q, D370Q and E372Q in the α-subunit of the cGMP-gated channel were introduced by polymerase chain reaction (Herlitze & Koenen, 1990). All mutations were verified by sequencing of the inserted fragment (Sanger, Nicklen & Coulson, 1977). mRNAs specific for WT and

mutant channels were synthesized *in vitro* (Melton, Krieg, Rebagliati, Maniatis, Zinn & Green, 1984). Synthesis was primed with m7G(5′)ppp(5′)G. The mRNA was injected into *Xenopus laevis* oocytes (H. Kähler, Institut für Entwicklungsbiologie, Hamburg, Germany; Centre National de la Recherche Scientifique, Montpellier, France) and oocytes were treated as described in Nizzari *et al.* (1993).

Solutions

The solution filling the patch pipette was composed of 2·5, 5, 10, 20, 50, 110 or 500 mM of the tested monovalent cation, 2 mM EDTA and 10 mM Hepes buffered to pH 7·6 with tetramethylammonium (TMA) hydroxide. Solutions were usually changed in the medium bathing the cytoplasmic side of the membrane. A cGMP-activated current was induced by adding 100 or 500 μM cGMP (sodium salt from Sigma, G-6129) at the cytoplasmic side of the membrane. In experiments in which the concentration of the tested monovalent cation was lower than 10 mM, the acid form of cGMP was used (Sigma, G-7504). In some experiments in which the $I-V$ relations were measured in the presence of different amounts of the chloride salt on the cytoplasmic side of the membrane, the osmotic pressure was balanced with an appropriate amount of sucrose. The ionic strength could not be balanced because no chloride salt is known which is impermeant and does not block the channel: choline chloride, TEA-Cl and TMA-Cl block the cGMP-gated channel rather powerfully (Menini, 1990). In other experiments, the osmotic pressure was not balanced and different amounts of the chloride salt were added to a solution containing only the Ca^{2+} and pH buffer. The $I-V$ relations measured when the osmotic pressure was balanced and when it was not differed by less than 10%.

The ionic activity of monovalent cations in the various solutions was obtained from the concentration of the dissolved salts and from the activity coefficients at the given temperature (Weast, 1986). The activity of solutions containing a concentration of 2·5, 5, 10, 20, 25, 50, 110, 250 and 500 mM NaCl was 2·5, 5, 10, 19, 24, 43, 85, 180 and 370 mM, respectively. The activity of solutions containing a concentration of 2·5, 5, 10, 20, 25, 50, 110, 250 and 500 mM LiCl was 2·5, 5, 10, 19, 24, 44, 87, 185 and 380 mM, respectively. The perfusion chamber had ten pipes through which different solutions flowed, so that the ionic medium bathing the cytoplasmic side of the membrane could be rapidly changed. The solution filling the patch pipette was not changed during a recording from the same patch.

Liquid junction potentials

The voltage offset between the extracellular and intracellular side of the membrane was routinely zeroed in the presence of a symmetrical solution on both sides of the membrane. Liquid junction potentials were measured as described in Menini (1990). Experimental measurements of liquid junction potentials were also compared with available theoretical equations. The liquid junction potential at the interface between two solutions of the same salt but with an activity a_1 and a_2 is:

$$V_d = (1 - 2t_{-1}) \frac{RT}{F} \ln \frac{a_1}{a_2}, \quad (1)$$

where R is the gas constant, T the absolute temperature, F the Faraday constant and t_{-1} the transport number (Gerasimov, 1974). For LiCl, NaCl, KCl, RbCl, CsCl and NH_4Cl, the transport numbers at 25 °C and at a concentration of 0·1 M are 0·32, 0·385, 0·49, 0·5, 0·5 and 0·49, respectively. The liquid junction potential was measured according to the method of Baylor & Nunn (1986) and was −2 mV between a patch pipette filled with 110 mM NaCl and the bathing medium with 110 mM LiCl and less than 1 mV for all the other monovalent cations. In these cases, the liquid junction potential was not compensated for and the $I-V$ relations were not corrected. From eqn (1), the liquid junction potentials between patch pipettes filled with 110 mM NaCl and bathing media containing 25, 50, 250 and 500 mM NaCl were 8, 4, −4 and −8 mV, respectively, and the liquid junction potentials between patch pipettes filled with 110 mM LiCl and bathing media containing 25, 50, 250 and 500 mM LiCl were 16, 8, −8 and −16 mV, respectively. The measured liquid junction potentials and those obtained from eqn (1) were usually similar to within 2 mV. When the absolute value of the junction potentials was larger than 2 mV, the $I-V$ relations were appropriately corrected.

Determination of $I-V$ relations

The cGMP-gated current was determined as the difference between a current recording in the presence of 100 μM cGMP and in its absence. The $I-V$ relation of the current activated by 100 μM cGMP was measured either with voltage ramps or with brief voltage pulses. Figure 1*B* illustrates the $I-V$ relations obtained by ramping the voltage from −100 to 100 mV and from 100 to −100 mV in 2 s. The two $I-V$ relations superimpose perfectly. Figure 1*C* reproduces current recordings obtained by stepping the voltage from the holding potential of 0 mV to ± 20, 60 and 100 mV. The $I-V$ relation measured at the steady state (i.e. by computing the mean value of the current between 20 and 300 ms) obtained from the experiment shown in Fig. 1*C* is superimposed (□) in Fig. 1*B*. There is good agreement between the $I-V$ relations measured with voltage ramps and with voltage pulses (□) in Fig. 1*B*.

$I-V$ relations from voltage ramps were obtained from the mean of at least two individual ramps. In experiments aimed at determining the reversal potential under bi-ionic conditions, at least five individual ramps were averaged. The $I-V$ relations obtained in the presence of 100 or 500 μM cGMP did not differ by more than 5%, suggesting that in the presence of 100 μM cGMP the open probability of the cGMP-gated channel was maximal.

The gating of the cGMP-gated channel has been shown to be voltage and time dependent (Karpen, Zimmerman, Stryer & Baylor, 1988). This voltage dependence is significant at low cGMP concentration (i.e. below 50 μM), but becomes negligible in the presence of a saturating cGMP concentration (i.e. 100 μM or more). Kaupp *et al.* (1989) for the heterologously expressed α-subunit, and Zimmerman & Baylor (1992) for the native channel, have shown that the shape of the $I-V$ relations in the presence of saturating cGMP concentrations is primarily determined by the voltage dependence of ion permeation and that the voltage dependence of channel gating accounts for only a small additional contribution (see Fig. 6 of Zimmerman & Baylor, 1992 and Fig. 6*C* in Kaupp *et al.* 1989). An analysis of the statistical properties of the flickering behaviour of a single channel in a rod inner segment (Sesti *et al.* 1994), in the presence of 100 μM cGMP, did not show any evident difference in the open probability at positive and negative membrane voltages (see the data shown in Fig. 2 of Sesti *et al.* 1994, where the amplitude histograms in *C* and *D* are fitted with the same β distribution, but with a different single-channel current). The closed probability of the WT channel expressed in oocytes in the presence of 100 μM cGMP was very similar, at −80 and +80 mV (see histograms in panel *B* of Fig. 1 of Nizzari *et al.* 1993). In addition, no evident effect on the open probability was observed when Na^+ was replaced with other monovalent cations, either in the native channel (Sesti *et al.* 1994) or in the WT channel

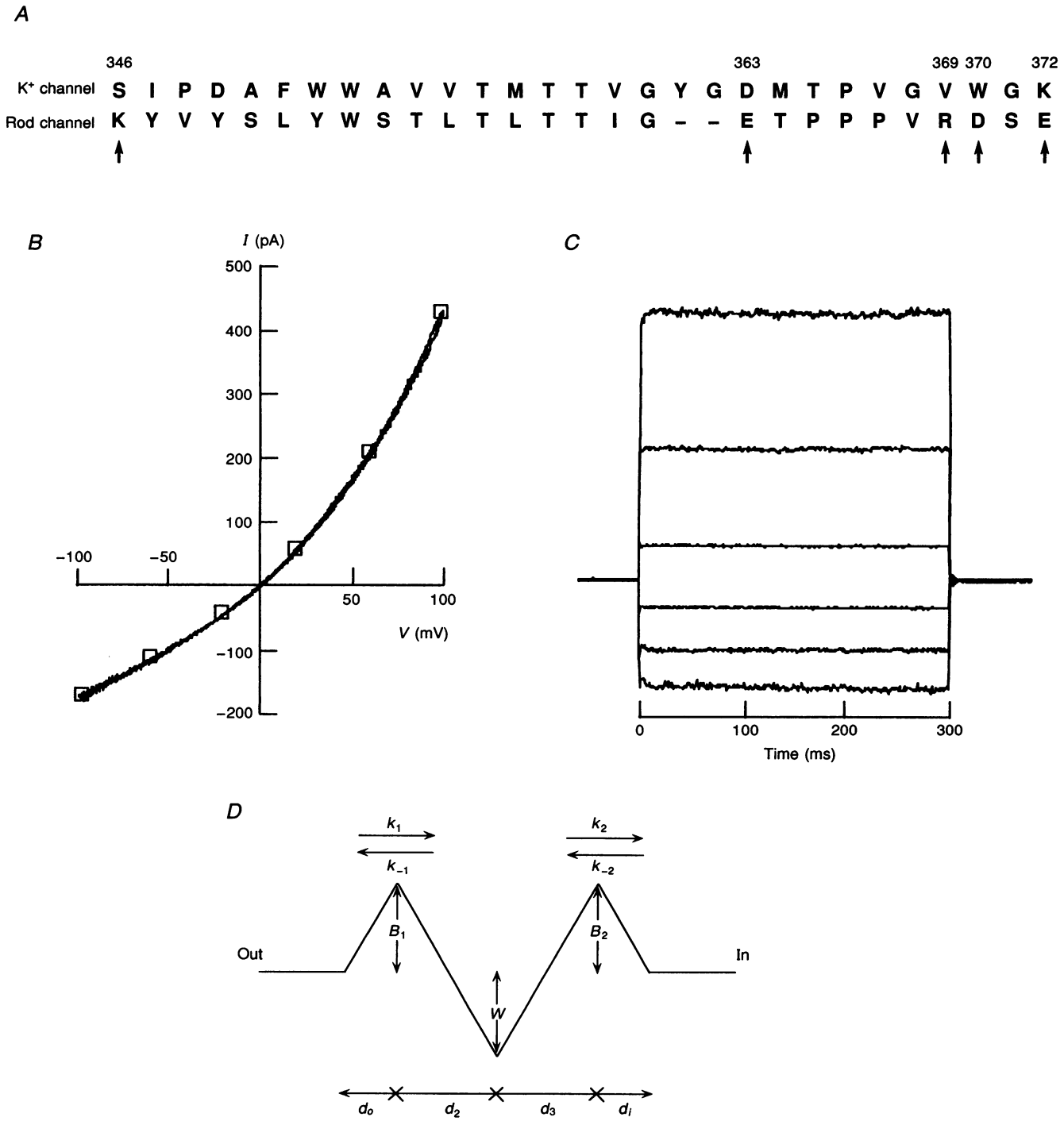

Figure 1. Determination of *I–V* relation with voltage ramps and with pulses

A, amino acid sequences of the putative region of a *shaker* K^+ channel and the cGMP-gated channel (Eismann *et al.* 1994). Amino acid residues are given in one-letter code; mutated amino acids are indicated. *B*, *I–V* relations obtained by ramping the voltage, under voltage-clamp conditions, from −100 to +100 mV and from +100 to −100 mV in 2 s. The two *I–V* relations superimpose perfectly. *C*, current recordings obtained by stepping the voltage from the 0 mV holding potential to ± 20, 60 and 100 mV. The *I–V* relation obtained from the experiment shown in *C* is superimposed (□) onto the voltage ramps in *B*. The current scale in *B* and *C* is the same. *D*, the Gibbs energy profile through the channel pore with two barriers (B_1 and B_2) and one well (*W*). d_o, d_2, d_3 and d_i are the equivalent electrical distances of barriers and well. k_1, k_{-1}, k_2 and k_{-2} are the transition rates through the barriers as indicated in the figure.

(Nizzari *et al.* 1993). For these reasons we have assumed that the shape of the $I-V$ relation of the macroscopic current determined with voltage ramps or with voltage steps (see Fig. 1) to a first approximation has the same shape as the $I-V$ relation of a single open channel.

One binding site

This section recalls well-known properties of the ionic permeation through a pore with a single binding site (Hille, 1992). In this case, the ionic permeation can be described, as in Fig. 1*D*, by a Gibbs free energy profile with two barriers and one well, which can be occupied by at most one single ion at any time. v is the voltage difference between the outside and inside of the membrane and the parameters of the model are the equivalent electrical distances d_o, d_2, d_3 and d_i, the barrier heights B_1 and B_2 and the well depth W. Electrical distances, barrier heights and well depth are different for the various ions; d_{io}, d_{i2}, d_{i3} and d_{ii} are the equivalent electrical distances and B_{i1}, B_{i2} and W_i are the barrier heights and well depth for the ionic species i. The transition rates k_{i1}, k_{i-1}, k_{i2} and k_{i-2} for the ionic species i in the extracellular medium are related to the different parameters of the model as:

$$k_{i1} = v\exp\left(\frac{-B_{i1}}{RT} - d_{io}V\right) \qquad k_{i-1} = v\exp\left(\frac{-(B_{i1}+W_i)}{RT} + d_{i2}V\right)$$

$$k_{i2} = v\exp\left(\frac{-(B_{i2}+W_i)}{RT} - d_{i3}V\right) \qquad k_{i-2} = v\exp\left(\frac{-B_{i2}}{RT} + d_{ii}V\right), \tag{2}$$

and similarly for the ionic species j in the intracellular medium the transition rates h_{j1}, h_{j-1}, h_{j2} and h_{j-2} are:

$$h_{j1} = v\exp\left(\frac{-B_{j1}}{RT} - d_{jo}V\right) \qquad h_{j-1} = v\exp\left(\frac{-(B_{j1}+W_j)}{RT} + d_{j2}V\right)$$

$$h_{j2} = v\exp\left(\frac{-(B_{j2}+W_j)}{RT} - d_{j3}V\right) \qquad h_{j-2} = v\exp\left(\frac{-B_{j2}}{RT} + d_{ji}V\right), \tag{3}$$

where $V = Fv/RT$, F is the Faraday constant and $v = kT/h$. The current I flowing in the presence of n different ionic species on the extracellular side and m different ionic species on the intracellular side is well known (Hille, 1992) to be:

$$I = \frac{\sum_i^n \frac{I_i[\mathrm{X}_i]}{K_i} - \sum_j^m \frac{I_j[\mathrm{Y}_j]}{H_j}}{1 + \sum_i^n \frac{[\mathrm{X}_i]}{K_i} + \sum_j^m \frac{[\mathrm{Y}_j]}{H_j}}, \tag{4}$$

where

$$I_i = -qz_iFk_{i-1} \qquad I_j = -qz_jFh_{j2}$$

$$K_i = \frac{k_{i-1}+k_{i2}}{k_{i-2}} \qquad H_j = \frac{h_{j-1}+h_{j2}}{h_{j1}},$$

q is the electron charge, z_i the ion valency, $[\mathrm{X}_i]$ the activity of the ionic species X_i in the extracellular medium and $[\mathrm{Y}_j]$ the activity of the ionic species Y_j in the intracellular medium.

In the presence of an identical concentration [X] of the same monovalent ionic species X on both sides of the membrane, eqn (4) simplifies to:

$$I = -qF\left(\frac{[\mathrm{X}]}{1 + [\mathrm{X}](k_1+k_{-2})/(k_2+k_{-1})}\right)\left(\frac{k_{-1}k_{-2}-k_1k_2}{k_{-1}+k_2}\right). \tag{5}$$

In the case of a symmetrical channel with a single binding site (with $B_1 = B_2 = B$), Bormann, Hamill & Sakmann (1987) have provided a simple and useful relation linking the single channel conductance γ (at 0 mV) to the barrier height B, well depth W and ionic activity [X]:

$$\gamma = \frac{1}{2}v[\mathrm{X}]\frac{F}{RT}\frac{\exp\{-(B+W)/RT\}}{[\mathrm{X}] + \exp(-W/RT)}. \tag{6}$$

Given a well depth of about $1{\cdot}4RT$, a single-channel conductance of about 60 pS is obtained from eqn (6) with a barrier height of about $10RT$. Therefore a value of $10RT$ is assumed to be the initial estimate for the barrier heights for Na^+. The values of B_1, B_2 and W for Na^+ were chosen so as to obtain a good fit of $I-V$ relations in the presence of different amounts of Na^+ (see Fig. 2*B*) and to give a single-channel conductance of 60 pS in the presence of 110 mM NaCl on both sides of the membrane (Sesti *et al.* 1994). The final choice for the three parameters was obtained manually and provided the values of 10·3, 9·7 and $1{\cdot}4RT$ for B_1, B_2 and W, respectively. The heights of barriers and well depth for Li^+ were chosen so as to fit the $I-V$ relations in the presence of different amounts of Li^+ and the measured bi-ionic reversal potential with Li^+ and Na^+.

RESULTS

As discussed in Methods, the shape of the $I-V$ relation of the macroscopic current measured in the presence of saturating cGMP concentrations (100 μM for the native channel and 500 μM for the WT channel) is assumed to be primarily caused by the intrinsic properties of the channel pore, and its shape therefore represents the $I-V$ relation of a single open channel. In this paper, the terms 'WT channel' and 'α-subunit' are used for the heterologously expressed homo-oligomeric WT α-subunit, while 'native channel' refers to the presumably hetero-oligomeric channel expressed in rods.

The $I-V$ relation of the native channel in the presence of different amounts of Na^+ or Li^+

It is useful to investigate to what extent the simple model of the channel with a single binding site is able to account for the permeation of monovalent cations. For this purpose, we analysed the $I-V$ relations in the presence of different amounts of the same permeating ion. Figure 2*A* shows the $I-V$ relations obtained in the presence of 110 mM Na^+ in the patch pipette and 25 (△), 50 (×), 110 (◇), 250 (+) and 500 (□) mM Na^+ in the bathing medium. The continuous lines through the symbols were obtained from eqn (4) with values for the electrical distances d_o, d_2, d_3, and d_i of 0·1, 0·38, 0·38 and 0·14, respectively, and for the barrier heights and well depth of 10·3, 9·7 and $1{\cdot}4RT$, respectively. These values were chosen so as to fit the experimental $I-V$ of Fig. 2*A* and to give a single-channel conductance of 60 pS at +60 mV (see Sesti *et al.* 1994) in the presence of symmetrical amounts of 110 mM NaCl.

When the same analysis was repeated with Li^+, a similar result was obtained. Figure 2*B* shows the $I-V$ relations

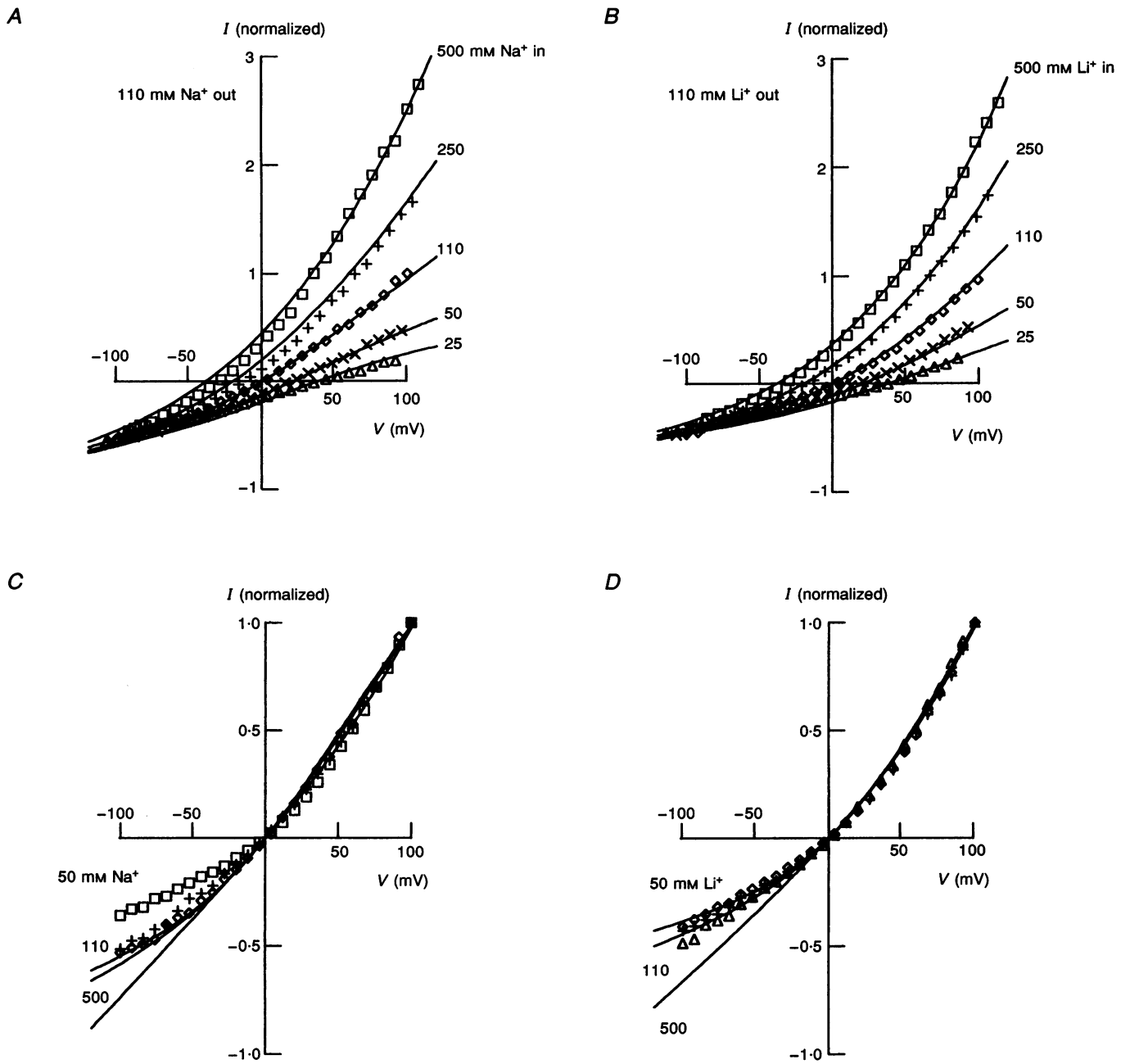

Figure 2. The *I–V* relation of the native channel in the presence of different amounts of Na^+ or Li^+

A and *B*, *I–V* relations in the presence of 110 mM Na^+ (*A*) and 110 mM Li^+ (*B*) in the patch pipette and in the presence of 25 (△), 50 (×), 110 (◇), 250 (+) and 500 (□) mM Na^+ (*A*) and Li^+ (*B*) in the bathing medium. The current flowing at +100 mV in the presence of 110 mM Na^+ and Li^+ was 475 and 310 pA, respectively, and was normalized to 1. *C* and *D*, *I–V* relations in the presence of symmetrical 50 (□), 110 (+) and 500 (◇) mM Na^+ (*C*) and 50 (◇), 110 (+) and 500 (△) mM Li^+ (*D*) on both sides of the patch membrane. Theoretical curves in *A* and *B* were obtained from eqn (4) and in *C* and *D* from eqn (5). In *A* and *C*, the electrical distances d_o, d_2, d_3 and d_i were 0·1, 0·38, 0·38 and 0·14, respectively, and the barrier heights B_1 and B_2 and well depth W were 10·3, 9·7 and 1·4RT, respectively. In *B* and *D*, the electrical distances d_o, d_2, d_3 and d_i were 0·1, 0·36, 0·36, 0·18 and B_1, B_2 and W were 10·25, 9·3 and 1·4RT, respectively (T was 298 °K). In *C* and *D*, experimental and theoretical *I–V* relations were normalized to the current flowing at +100 mV. The ionic activity [X] of the different solutions was that specified in Methods. The parameter values used to fit the *I–V* relations of panel *A* provide a single-channel conductance of 60 pS at +60 mV.

obtained in the presence of 110 mM Li^+ in the patch pipette and 25 (△), 50 (×), 110 (◇), 250 (+) and 500 (□) mM Li^+ in the bathing medium. The continuous lines through the symbols were obtained from eqn (4) with the values for the electrical distances d_o, d_2, d_3, and d_i of 0·1, 0·36, 0·36 and 0·18, respectively, and for barrier heights and well depth of 10·25, 9·3 and $1{\cdot}4RT$, respectively. The barrier heights were adjusted so as to reproduce the reversal potential in bi-ionic conditions in which 110 mM NaCl or LiCl were present at each side of the membrane, which was +4 or −4 mV depending on whether Na^+ was inside or outside the patch pipette.

A particular feature of the I–V relations shown in Fig. 2*A* and *B* is that the degree of saturation observed when the ionic concentration was increased is about the same for Li^+ and Na^+. This behaviour was also seen when the patch pipette was filled with 500 mM amounts of the chloride salt and the osmotic pressure of the bathing medium was balanced with appropriate amounts of sucrose. Whether or not the osmotic pressure was balanced with sucrose in the patch pipette or the bathing medium caused very little change in the results of the experiments illustrated in Fig. 2*A* and *B*.

The good agreement between the model and the experimental I–V relations confirms the proposal of Menini (1990) and Zimmerman & Baylor (1992) that a simple model with two barriers and a well is adequate to describe many features of ionic permeation through the native cGMP-gated channel. It is important, however, to test whether this simple model is able to reproduce other experimental results.

Figure 2*C* reproduces normalized I–V relations obtained in the presence of 50 (□), 110 (+) and 500 (◇) mM NaCl on both sides of the membrane patch. As was expected from the simple model shown in Fig. 1*C*, the shape of the I–V relation changes with the ionic activity. The continuous lines through the experimental points were obtained from eqn (5) with the same parameter values used to fit the I–V relations in Fig. 2*A*. Figure 2*D* reproduces normalized I–V relations obtained in the presence of 50 (◇), 110 (+) and 500 (△) mM LiCl on both sides of the membrane patch. In the presence of Li^+, the shape of the I–V relation did not change significantly with the ionic activity. The continuous lines through the experimental points were obtained from eqn (5) with the same parameter values used to fit the I–V relations in Fig. 2*B*. The fitting of the experimental I–V relations of Fig. 2*C* and *D* with the simple model of Fig. 1*D* is not very satisfactory. A better, but not perfect, fitting could be obtained by not constraining the two electrical distances d_2 and d_3 to be equal.

The I–V relations of the native channel in the presence of two ionic species

An obvious test for the simple model of ionic permeation illustrated in Fig. 1*D* with only one binding site is to compare the predictions of the model with the I–V relations obtained in the presence of two different ionic species on the two sides of the membrane patch. This test is particularly interesting with Na^+ and Li^+ because, as shown in the previous section, the well depth for both ions is about the same and the barrier heights differ by less than $0{\cdot}3RT$. As a consequence these two ions are expected to carry a similar maximal current. Figure 3*A* illustrates the I–V relations obtained with the patch pipette filled with 110 mM Na^+ and in the presence of 110 mM Na^+ (◇) or 110 mM Li^+ (+) in the bathing medium. Similarly, Fig. 3*B* shows the I–V relations obtained with the patch pipette filled with 110 mM Li^+ and in the presence of 110 mM Na^+ (◇) or 110 mM Li^+ (+) in the bathing medium. In all cases the outward current carried by Li^+ was about three times smaller than that carried by Na^+, which is not in agreement with the simple model of one single site with fixed parameters. The continuous line through the experimental I–V relations in Fig. 3*A* was obtained with the same parameter values used to fit the I–V relations in Fig. 2*A* and *B*, with the exception of the well depth for Li^+, which was set equal to $4{\cdot}2RT$. The value of the well depth for Li^+ necessary to fit the I–V of Fig. 3*A* was at least 2-fold larger than the well depth necessary to fit the I–V relations of Fig. 2*A*.

Figure 3*C* reproduces the I–V relations measured with the patch pipette filled with 110 mM Na^+ and in the presence of 25 (△), 50 (×), 110 (◇), 250 (+) and 500 (□) mM Li^+. Even in the presence of Na^+ in the patch pipette, increasing the Li^+ concentration in the bathing medium produced only a moderate saturation of the current carried by Li^+. These I–V relations could be fitted with eqn (4) and the values used to fit the I–V relations of Fig. 2, provided that the well depth for Li^+ decreased when the Li^+ concentration was increased from 25 to 500 mM.

Figure 3*D* illustrates the dependence of the current flowing at +90 mV as a function of the intracellular Li^+ activity in the presence of 110 mM Li^+ (open symbols) or Na^+ (filled symbols) in the patch pipette. The amplitude of the current increased with the Li^+ activity in the intracellular medium and showed some saturation when the Li^+ activity was increased to more than 100 mM, consistent with a well depth between 1 and $2RT$.

Determination of the low activity range

The experimental results reported in Figs 2*B* and 3*D* indicate a well depth for Li^+ between 1 and $2RT$, while the data reproduced in Fig. 3*A* and *B* suggest a much deeper well depth in the order of $4RT$. As a consequence, in the presence of 110 mM Li^+, a well depth of $4RT$ is consistent with a channel almost completely saturated by Li^+, while with a well depth between 1 and $2RT$, the channel is only moderately occupied by Li^+. In order to resolve this apparent discrepancy, the Li^+ activity for which the occupancy of the channel is small must be determined. In

the presence of equimolar amounts of Li^+ and Na^+ at the two sides of the membrane, the reversal potential is only a few millivolts (Menini, 1990), indicating that the permeability ratio between Na^+ and Li^+ is close to 1. It is well known that in the low activity range, when the channel is rarely occupied, the permeability ratio becomes similar to the conductance ratio. Therefore the low activity range for Li^+ can be determined by analysing at which ionic activity the conductance ratio becomes similar to the permeability ratio.

Figure 4 illustrates the results of experiments in which the patch pipette was filled by a Li^+ concentration between 2·5

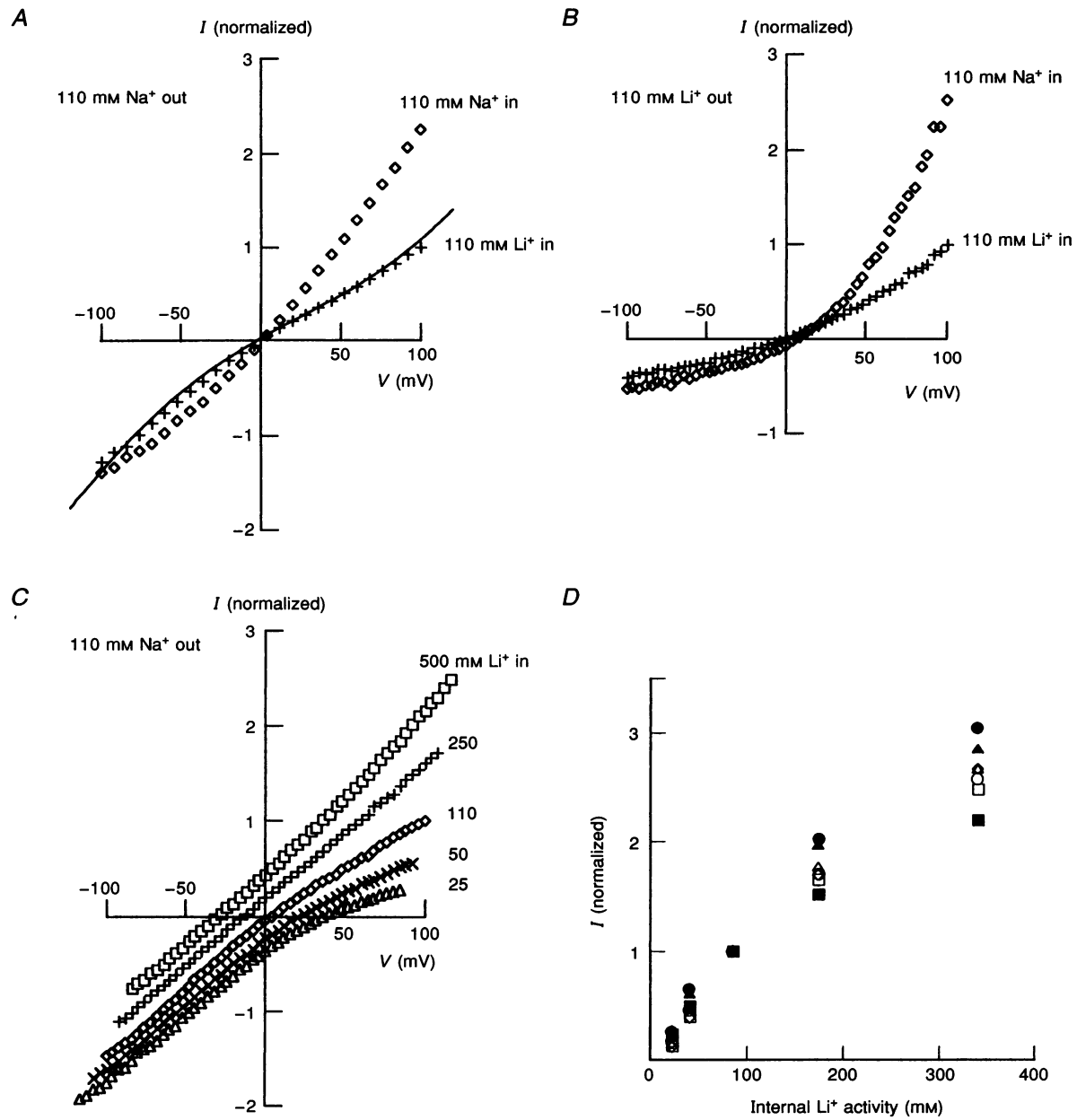

Figure 3. The *I–V* relation of the native channel in the presence of Na^+ and Li^+

A and *B*, 110 mM NaCl (*A*) and LiCl (*B*) in the patch pipette and in the presence of 110 mM NaCl (◇) and LiCl (+) in the bathing medium. The continuous line was obtained from eqn (4) with the same parameter values used to fit the *I–V* relations in Fig. 2 with the exception that the well for Li^+ was set equal to 4·2*RT*. *C*, *I–V* relations in the presence of 110 mM Na^+ in the patch pipette and in the presence of 25 (△), 50 (×), 110 (◇), 250 (+) and 500 mM Li^+ (□) in the bathing medium. Currents in *A*, *B* and *C* flowing at +100 mV in the presence of 110 mM LiCl in the bathing medium were 280, 170 and 198 pA, respectively, and were normalized to 1. *D*, the relation between the current carried by Li^+ at +90 mV and the Li^+ activity in the bathing medium in the presence of 110 mM Li^+ (open symbols) or 110 mM Na^+ (filled symbols) in the patch pipette.

and 50 mM and the bathing medium contained an equimolar amount of Li^+ (+) or Na^+ (◇). As shown in *A*, *B* and *C* in the presence of 50, 10 and 2·5 mM Li^+, the ratio between the current carried at +100 mV by Na^+ and Li^+ was 2·2, 1·7 and 1·3, respectively. Figure 4*D* reproduces the ratio between the current carried by equimolar amounts of Na^+ and Li^+ at +100 mV as a function of the Li^+ activity in the patch pipette. This ratio was 2·3 at the usual concentration of 110 mM and decreased to 1·3 at a concentration of 2·5 mM. Therefore the permeability ratio and the conductance ratio become similar when the ionic activity is below 5 mM. This result indicates that even in the presence of only 5 or 10 mM Li^+, the native cGMP-gated channel is significantly occupied by Li^+, suggesting a high affinity for Li^+ consistent with a well depth of at least $4RT$.

The permeation of Li^+ through the native cGMP-gated channel seems to be more complicated than previously expected and cannot be explained by a simple single-site model with a fixed well. The depth of the well for Li^+ appears to depend on the Li^+ concentration in the perfusate: increasing the Li^+ concentration causes a reduction of the well depth. This behaviour is predicted by the existence of a high-affinity binding site for Li^+ within the channel, whose affinity decreases in the presence of larger amounts of Li^+. This behaviour is similar to the permeation of Ca^{2+} through Ca^{2+} channels, where a similar transition from a high-affinity and a low-affinity site is observed when the channel occupancy is increased (Kuo & Hess, 1993*a*, *b*). The transition between a high-affinity binding site and a low-affinity binding site is usually explained as originating from a double occupancy of the

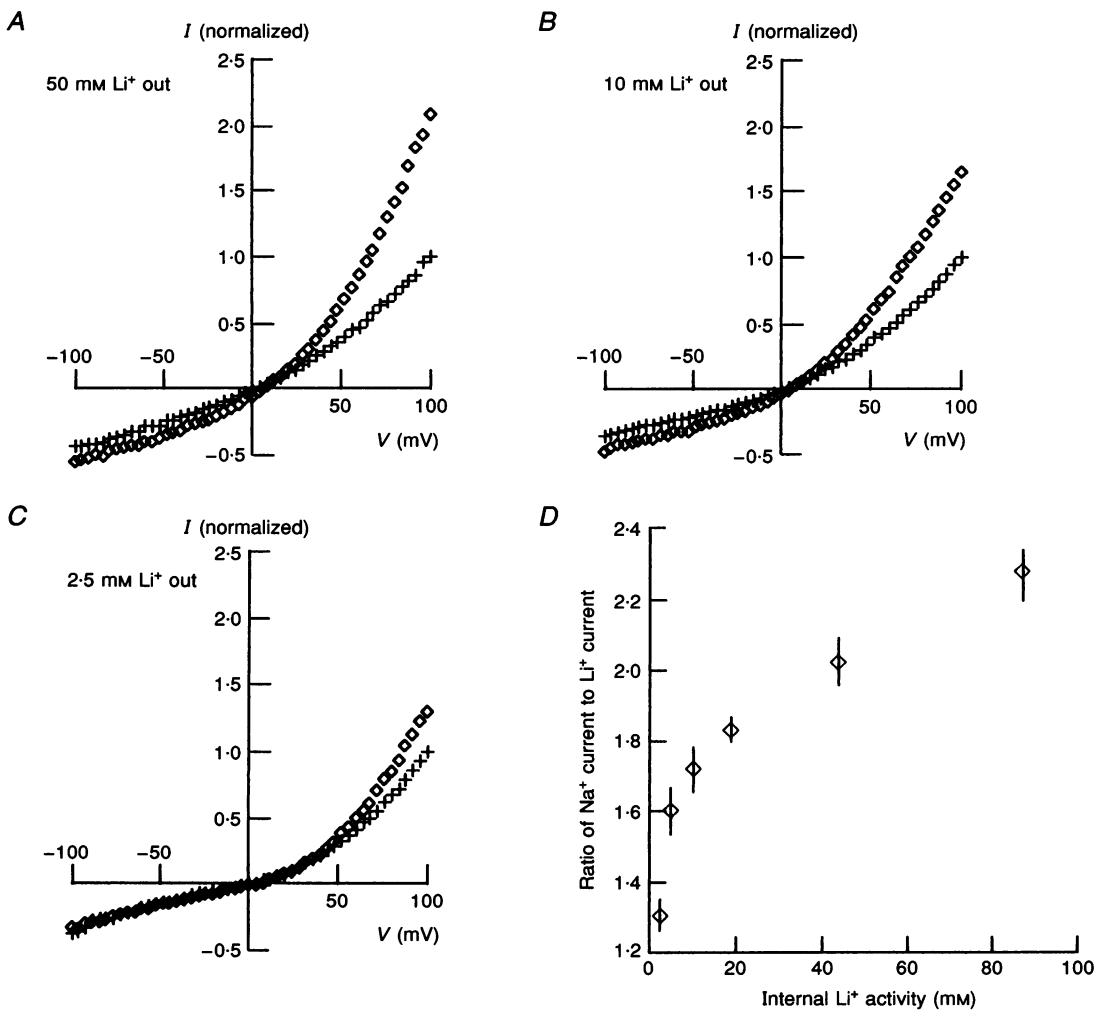

Figure 4. Determination of the low activity range for Li^+ in the native channel

In *A*, *B* and *C* the patch pipette contained 50, 10 and 2·5 mM Li^+ and the bathing medium contained an equimolar amount of Li^+ (+) or Na^+ (◇). The current flowing in the presence of symmetrical 50, 10 and 2·5 mM Li^+ at +100 mV was 150, 80 and 75 pA, respectively, and was normalized to 1. *D*, the relation between the ratio of the current flowing in the presence of Na^+ and Li^+ at +100 mV and the Li^+ activity inside the patch pipette. The vertical bars indicate the standard deviation of the ratio between the current carried by Na^+ and Li^+.

channel. As a consequence, these experiments suggest that two Li^+ can bind within the channel.

The dependence of reversal potential of the native channel on ionic activity

When the patch pipette was filled by 110 mM Na^+ and the bathing medium contained an equimolar amount of Li^+, K^+, Rb^+, Cs^+ and NH_4^+, the reversal potential was on average −4, 0, 8, 17 and −25 mV, respectively. In experiments in which 110 mM Na^+ was in the bathing medium and an equimolar amount of Li^+, K^+, Rb^+, Cs^+ and NH_4^+ was in the patch pipette, the reversal potential was on average 4, 0, −8, −16 and +26 mV. These values did not change significantly when the ionic activity inside the patch pipette was reduced to 50 and 20 mM. Furman & Tanaka (1990), however, reported some asymmetries of the reversal potential in frog and toad rods in the presence of the bi-ionic solutions NH_4^+–Na^+ and Cs^+–Na^+, which suggested that the native cGMP-gated channel in these rods was a multi-ion channel.

The anomalous mole fraction effect in the native channel in the presence of mixtures of Li^+ and Cs^+

Some of the experiments suggesting the simultaneous presence of two Li^+ ions within the channel were obtained under conditions in which the osmolarity and ionic strength were not kept constant. Therefore additional evidence must be obtained for the simultaneous presence of two ions

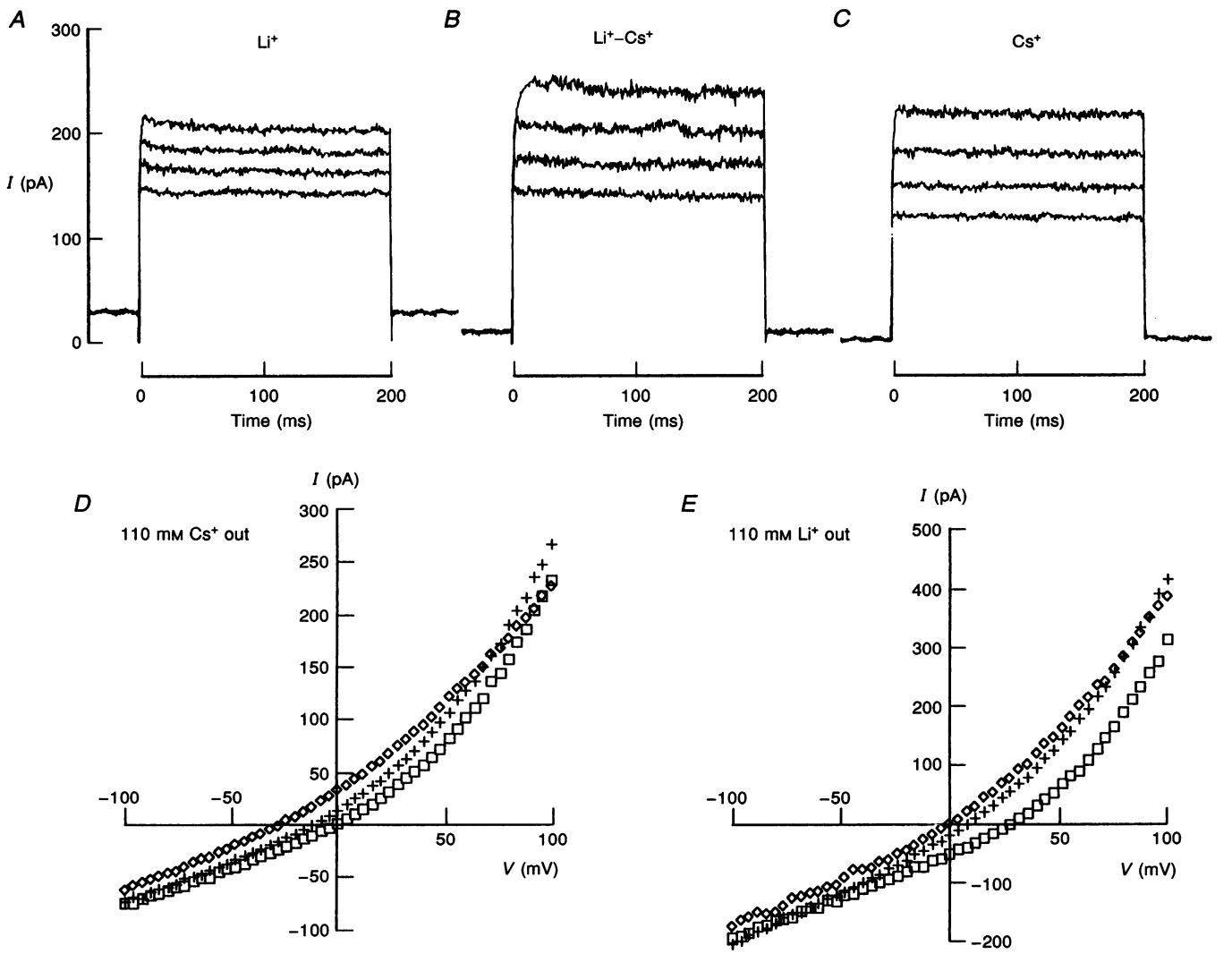

Figure 5. The *I–V* relation of the native channel in the presence of mixtures of Li^+ and Cs^+

Current recordings in response to voltage pulses from a holding voltage of 0 mV to +70, 80, 90 and 100 mV in the presence of 110 mM Cs^+ inside the patch pipette and 110 mM Li^+ (*A*), 55 mM Li^+ plus 55 mM Cs^+ (*B*) and 110 mM Cs^+ (*C*) in the bathing medium. *D*, *I–V* relations in the presence of 110 mM Cs^+ inside the patch pipette and 110 mM Cs^+ (□), 55 mM Li^+ and 55 mM Cs^+ (+), and 110 mM Li^+ (◇) in the bathing medium. *E*, *I–V* relations in the presence of 110 mM Li^+ inside the patch pipette and 110 mM Cs^+ (□), 33 mM Li^+ and 77 mM Cs^+ (+), and 110 mM Li^+ (◇) in the bathing medium.

within the pore when the osmolarity and the ionic strength did not vary.

A well-known result indicating the deviation from the simple one-site model of Fig. 1*D* is the anomalous mole fraction effect which can be observed in the presence of two permeating ions (Almers & McCleskey, 1984; Hess & Tsien, 1984). As can easily be seen from eqn (4), if x is the fraction of the permeating ion X and $1 - x$ is the fraction of the permeating ion Y, the model with only one site predicts that at a given voltage the total current carried by the two ionic species X and Y is an increasing or decreasing function of the molar fraction x. Deviations from this simple behaviour are assumed to be an indication of the simultaneous binding of at least two ions within the channel. The native cGMP-gated channel does not show any anomalous mole fraction effect in the presence of mixtures of Li^+ and Na^+ (Menini, 1990) and mixtures of Ca^{2+} and Na^+ (Zimmerman & Baylor, 1992). The anomalous mole fraction effect is likely to be more evident in the presence of a large and a small ion. Therefore this effect was analysed with mixtures of Li^+ and Cs^+.

Figure 5 illustrates current recordings obtained in the presence of voltage pulses from 0 to +70, 80, 90 and 100 mV in the presence of 110 mM Cs^+ in the patch pipette and 110 mM Li^+ (*A*), 55 mM Cs^+ and 55 mM Li^+ (*B*) and 110 mM Cs^+ (*C*) in the bathing medium. The current flowing in the presence of the mixture of Li^+ and Cs^+ (*B*) is clearly larger than the current flowing either with Cs^+ (*C*) or Li^+ (*A*) alone. The *I–V* relations obtained in the presence of either 110 mM Cs^+ or 110 mM Li^+ in the patch pipette are shown in panels *D* and *E*, respectively. At membrane voltages around 100 mV in both cases, the current carried by the Li^+–Cs^+ mixture (+) is larger than the current observed in the presence either of Li^+ (◇) or Cs^+ (□) only.

Figure 6 illustrates the mole fraction effect under various experimental conditions. In all panels the current measured at +100 mV was normalized to the current flowing in the absence of Cs^+. The anomalous behaviour could be observed with mixtures of Li^+ and Cs^+ with a total ionic concentration of 110 mM, with the patch pipette filled either by Cs^+ (*A*) or Li^+ (*B*). When the patch pipette was filled with Cs^+, the current carried by Cs^+ was about the same as the current carried by Li^+. In contrast, when the patch pipette was filled with Li^+, Li^+ carried a larger current than Cs^+. It is also useful to remark that the anomalous behaviour was reduced and even abolished at membrane voltages larger than +140 mV, when the current carried by Cs^+ increased very steeply with voltage. The anomalous behaviour could not be observed when the total ionic concentration on both sides of the patch was increased to 500 mM (*C*) or when Li^+ was replaced by NH_4^+ (*D*). In agreement with previous observations (Menini, 1990), no evident anomalous mole fraction effect could be observed with Na^+–Li^+ mixtures in the bathing medium and either Na^+, Li^+, K^+ or NH_4^+ in the patch pipette. The dependence of the reversal potential in the experiments shown in Figs 5 and 6 on the mole fraction x did not show any anomalous behaviour. When the patch pipette was filled with 110 mM Cs^+ and 110 mM Li^+ was in the bathing medium, the reversal potential was −22 mV and monotonically approached 0 mV as the fraction of Cs^+ in the bathing medium was increased.

Ionic permeation through the WT channel

The ionic permeation through the WT channel (Kaupp *et al.* 1989) has properties very similar, but not identical, to those of the native cGMP-gated channel in rods of the tiger salamander (Menini, 1990; Zimmerman & Baylor, 1992) or in bovine rods (Lühring *et al.* 1990). A noticeable difference is that the reversal potential in the presence of a bi-ionic solution with Na^+ outside and Li^+ inside is about −4 mV in the native channel and +8 mV in the WT channel.

Some other differences have emerged from the present analysis: the shape of the *I–V* relations of the WT channel in the presence of saturating concentrations of cGMP does not depend on the ionic species of the permeating ion, as in the native channel (data not shown). With the exception of these minor differences, the following sections show that ionic permeations through the native and the WT cGMP-gated channels are remarkably similar: they share the same properties characteristic of a multi-ion pore and have a similar affinity for monovalent cations. Therefore, in order to understand the molecular basis of the multi-ion nature of the cGMP-gated channel, it is necessary to analyse the electrical properties of mutant channels. As the pore region of the WT channel (see Fig. 1*A*) is supposed to be between lysine 346 and glutamate 372 (Eismann *et al.* 1994), we have studied mutant channels, where charged residues in this region were neutralized. In particular we have examined the replacement of lysine 346, glutamate 363, arginine 369, aspartate 370 and glutamate 372 with the neutral amino acid glutamine. In the case of glutamate 363, the replacements with aspartate and asparagine were also analysed. The mRNA of mutant and WT channels was injected into oocytes and cGMP-gated channels were studied in excised patches in the inside-out configuration.

The dependence of outward current of WT and mutant channel E363Q on intracellular ion activity

The outward current carried by intracellular monovalent alkali cations through the native cGMP-gated channel in vertebrate rods increases when the activity of these ions is elevated in the intracellular medium (Menini, 1990; Zimmerman & Baylor, 1992; see also Fig. 3*D*). The outward current carried by Na^+, Li^+ and K^+ reached half of its maximal amplitude for ionic activities around 200 mM.

The ion permeation through the heterologously expressed WT α-subunit of the cGMP-gated channel showed a very similar behaviour. As shown in Fig. 7*A*, the outward

current at +90 mV carried by 500 mM Na^+ was about twice the current carried by 110 mM Na^+. The dependence of the outward current at +90 mV on the Na^+ activity at the cytoplasmic side is shown in Fig. 7*C*, where triangles and diamonds refer to the native and WT channel, respectively. The outward current in both channels had a similar half-maximal amplitude around 200 mM Na^+. Similar results were obtained in both channels when the permeating ion was Li^+. A different behaviour was observed for the mutant channel E363Q. As shown in Fig. 7*B*, the outward current carried by 500 mM Na^+ at +90 mV was about 4 times the current carried by 110 mM Na^+. The dependence of the outward current on the Na^+ activity at the cytoplasmic side is reproduced in Fig. 7*D*. Unlike the native and WT channels, no sign of current saturation was detected and the experimental points could be fitted by a straight line, indicating that the mutant channel E363Q has a very low affinity for Na^+ (and Li^+, data not shown).

The anomalous mole fraction effect with mixtures of Li^+ and Cs^+ in WT and mutant channel E363Q

As shown in the previous section, an anomalous mole fraction behaviour was observed in the native channel when the patch pipette was filled with 110 mM Cs^+ or Li^+ and in the presence of mixtures of 110 mM of Li^+ and Cs^+ in the bathing medium. A similar behaviour was observed in the WT channel: the outward current carried by 33 mM Cs^+ and 77 mM Li^+ was larger than the current carried by either 110 mM Cs^+ or Li^+ (see Fig. 8*A*). The anomalous mole fraction effect was not observed in the mutant channel E363Q. As shown in Fig. 8*B*, the current carried by the

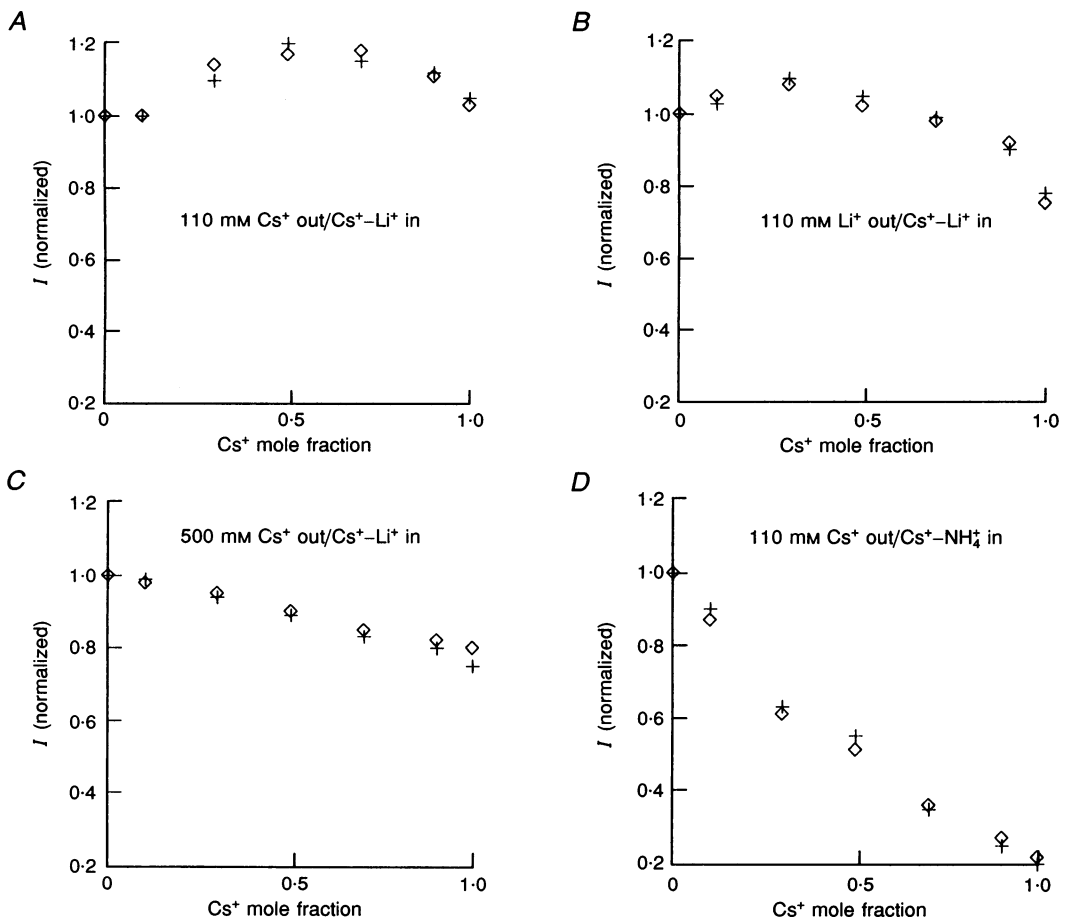

Figure 6. The amplitude of the current flowing at +100 mV in the presence of mixtures of Li^+–Cs^+ and Cs^+–NH_4^+ in the native channel

A, the current flowing in the presence of 110 mM Cs^+ in the patch pipette and mixtures of Li^+ and Cs^+ in the bathing medium. *B*, the current flowing in the presence of 110 mM Li^+ in the patch pipette and mixtures of Li^+ and Cs^+ in the bathing medium. *C*, the current flowing in the presence of 500 mM Li^+ in the patch pipette and mixtures of Li^+ and Cs^+ in the bathing medium. *D*, the current flowing in the presence of 110 mM Cs^+ in the patch pipette and mixtures of Cs^+ and NH_4^+ in the bathing medium. The current was normalized to the current flowing in the absence of Cs^+. The solutions bathing the cytoplasmic side of the patch had the same tonicity as the solutions inside the patch pipette. Different symbols indicate data obtained from different patches.

Cs^+–Li^+ mixture had an amplitude always intermediate between that measured with either 110 mM Cs^+ or Li^+.

The dependence of the amplitude of the outward current (at +90 mV) and of the reversal potential on the Cs^+ mole fraction is shown in Fig. 8*C* and *D*, respectively. In both panels, diamonds and triangles refer to the WT and mutant channel E363Q, respectively. The existence of an anomalous mole fraction effect on the reversal potential of the WT channel is relevant for two reasons. Firstly, it is an effect which does not depend on the number of open channels and constitutes, therefore, the best demonstration of the multi-ion nature of the cGMP-gated channel. Secondly, the native channel does not show an evident anomalous mole fraction effect on the reversal potential, and this difference has to be noted.

The mutant channels E363D and E363N

In previous sections it was shown that the anomalous mole fraction effect which was observed with mixtures of Li^+ and Cs^+, both in the native and WT channel, was abolished when glutamate 363 was neutralized with glutamine, which has dimensions very similar to glutamate. It is interesting, also, to examine the substitution of glutamate 363 for an aspartate for at least two reasons: firstly, aspartate and glutamate have very similar electrical properties but aspartate is a smaller amino acid and secondly, as shown in Fig. 1*A*, K^+ channels have an aspartate and not a

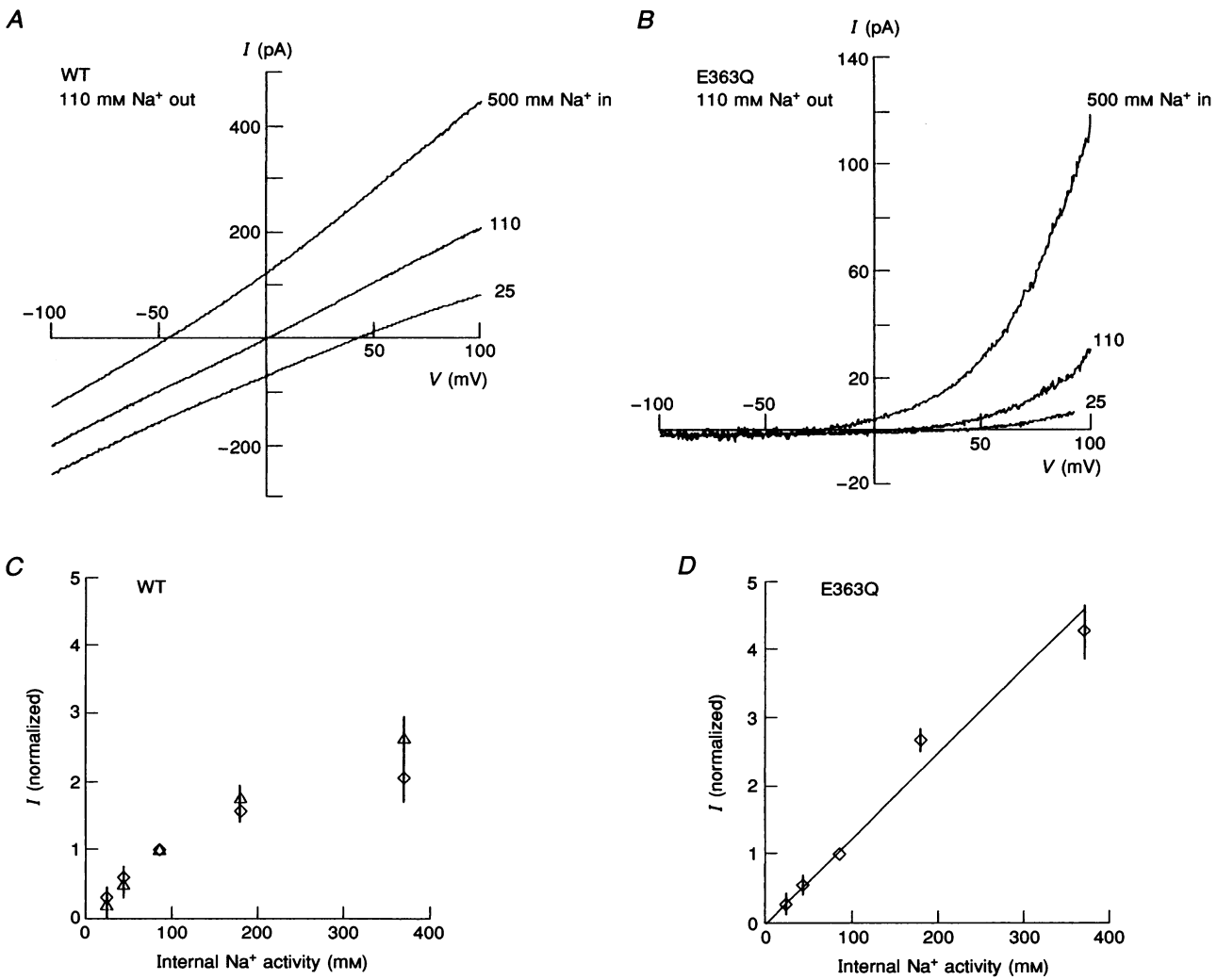

Figure 7. Dependence of the outward current on ion activity at the cytoplasmic side in the WT and mutant channel E363Q

A and *B*, *I–V* relations from WT channel and mutant channel E363Q respectively, activated by 500 μM cGMP. The patch pipette was filled with 110 mM Na^+ and the bathing medium contained 25, 110 or 500 mM Na^+. *C*, dependence of the outward current at +90 mV on Na^+ activity at the cytoplasmic side. △ and ◇ refer to the native channel and the WT, respectively. Current was normalized to the current carried by 110 mM Na^+. *D*, as in *C* but for mutant channel E363Q. Each point was obtained from at least 4 different patches. Vertical bars indicate the standard deviation of the mean value.

glutamate at the analogous position. In order to understand the role of size and charge of residues along the pore region it is instructive to see whether the substitution of the glutamate with a glutamine or an asparagine produces mutant channels with similar electrical properties.

The dependence of the outward current (at +90 mV) of the mutant channels E363D (◇) and E363N (+) on the internal Na^+ activity is illustrated in Fig. 9*A*, where for comparison the data of Fig. 7 relative to the WT (□) and mutant channel E363Q (×) are also reproduced.

The WT and mutant channel E363D differ also when various mixtures of Li^+ and Cs^+ are substituted in the medium bathing the intracellular side of the membrane. As shown in Fig. 9*B*, in the mutant channel E363D the outward current carried by Cs^+ at +100 mV is considerably larger than the current carried by Li^+, while the opposite behaviour was observed in the WT channel (Fig. 8*B*). It is also useful to observe that the shape of the *I–V* relation of the mutant channel E363D (Fig. 9*B*) in the presence of a symmetrical solution containing 110 mM Cs^+ has a clear outward rectification which is absent in the WT channel (see Fig. 8*A*). As illustrated in Fig. 9*C*, the anomalous mole fraction effect in the mutant channel E363D was observed at +30 mV (◆) and not at +100 mV (◇), but could be clearly detected when the reversal potential was measured

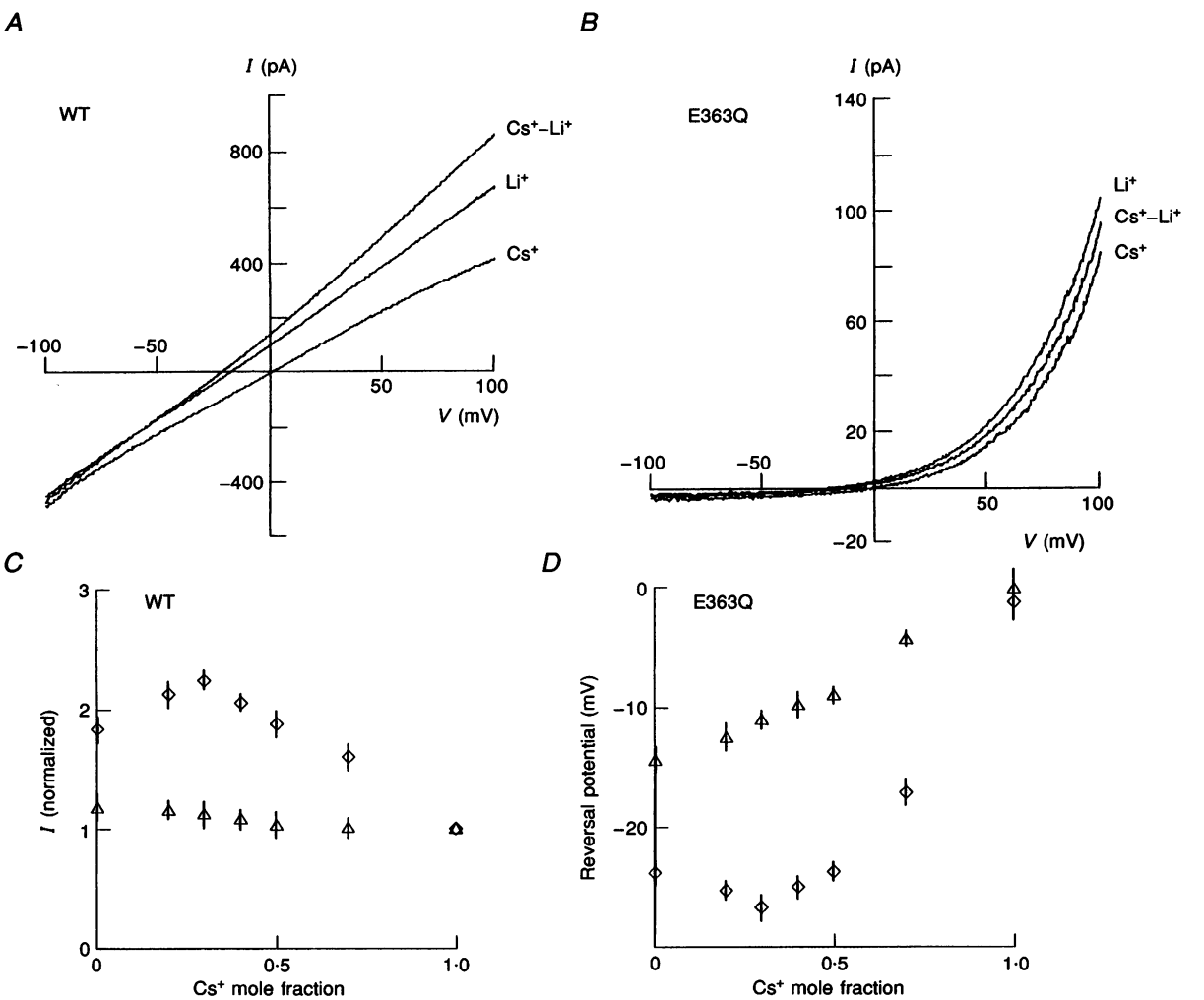

Figure 8. Anomalous mole fraction effect with mixtures of Li^+ and Cs^+ in the WT and mutant channel E363Q

A and *B*, *I–V* relations from WT and mutant channel E363Q, respectively. The patch pipette was filled with 110 mM Cs^+ and the bathing medium contained 110 mM Cs^+, 110 mM Li^+, or 33 mM Cs^+ plus 77 mM Li^+. *C*, dependence of the outward current at +100 mV on the Cs^+ mole fraction in the bathing medium. Current was normalized to the current measured in the absence of Li^+. *D*, dependence of the reversal potential on the Cs^+ mole fraction in the bathing medium. △ and ◇ refer to the WT and mutant channel E363Q, respectively. Each point was obtained from 5 patches excised from different oocytes. Vertical bars indicate the standard deviation. The current was activated by 500 μM cGMP.

(Fig. 9*D*). The anomalous mole fraction effect was not observed in the mutant channel E363N (△), as shown in Fig. 9*C* and *D*.

The multi-ion nature of the mutant channel E363D

The anomalous mole fraction effect with mixtures of Li^+ and Cs^+ observed in the native and WT channel is significantly reduced when glutamate 363 is substituted for aspartate and it is interesting to establish whether the mutant channel E363D is a multi-ion channel. As shown in Fig. 9*A*, the outward current carried by internal Na^+, both in the WT and mutant channel E363D, is half-activated by an ionic activity around 200 mM, indicating that both channels have a low affinity for monovalent cations. Therefore it is important to establish whether these channels, as with the native channel, exhibit the same transition between a high-affinity and a low-affinity binding site when the ionic concentration is increased.

Figure 10 illustrates *I–V* relations obtained in the presence of 2·5 (*A* and *D*) or 110 (*B* and *E*) mM Li^+ inside the patch pipette and an equimolar amount of Li^+ (+) or Na^+ (◇) in the bathing medium. Panels *A* and *B* refer to the WT channel, while panels *D* and *E* refer to the mutant channel E363D. In both channels, the amplitude of the outward current at +100 mV carried by 110 mM Na^+ was more than twice that carried by an equimolar amount of Li^+. In the presence of 2·5 mM, however, this ratio was significantly reduced and approached a value of around 1·4.

Figure 10*C* and *F* illustrates the dependence of the ratio between the outward current at +100 mV carried by Na^+ and Li^+ on the ionic activity for the WT and mutant

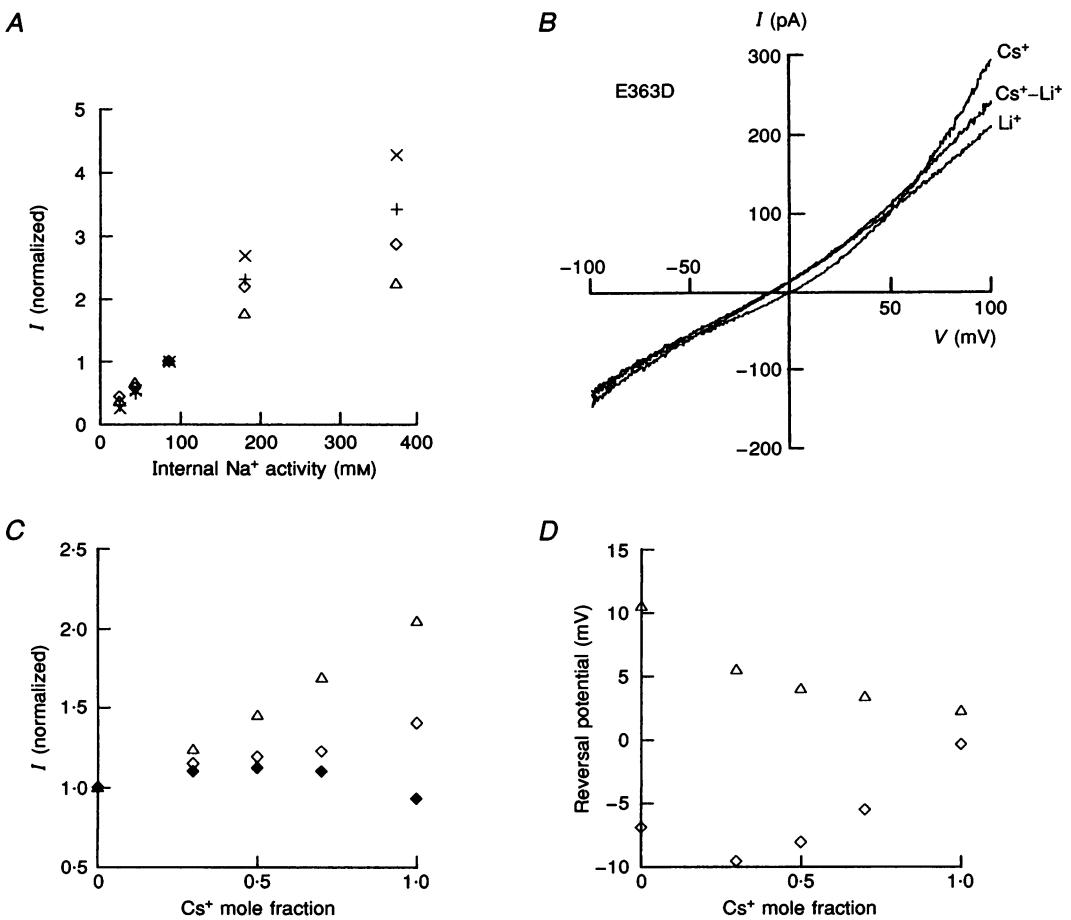

Figure 9. Electrical properties of mutant channels E363D and E363N

A, dependence of the outward current at +90 mV on the Na^+ activity at the cytoplasmic side for the WT (△) and mutant channels E363D (◇), E363Q (×) and E363N (+). Current normalized to the current flowing in the presence of 110 mM Na^+. *B*, *I–V* relations of the mutant channel E363D with the patch pipette filled with 110 mM Cs^+ and the bathing medium containing 110 mM Cs^+, 100 mM Li^+, or 33 mM Cs^+ plus 77 mM Li^+. *C*, dependence of the outward current at +30 (◆) and +100 mV (◇) on the Cs^+ mole fraction in the bathing medium. Currents were normalized to the current measured in the absence of Li^+. △ refers to the mutant channel E363N. *D*, dependence of the reversal potential on the Cs^+ mole fraction in the bathing medium. ◇ and △ refer to the mutant channels E363D and E363N, respectively.

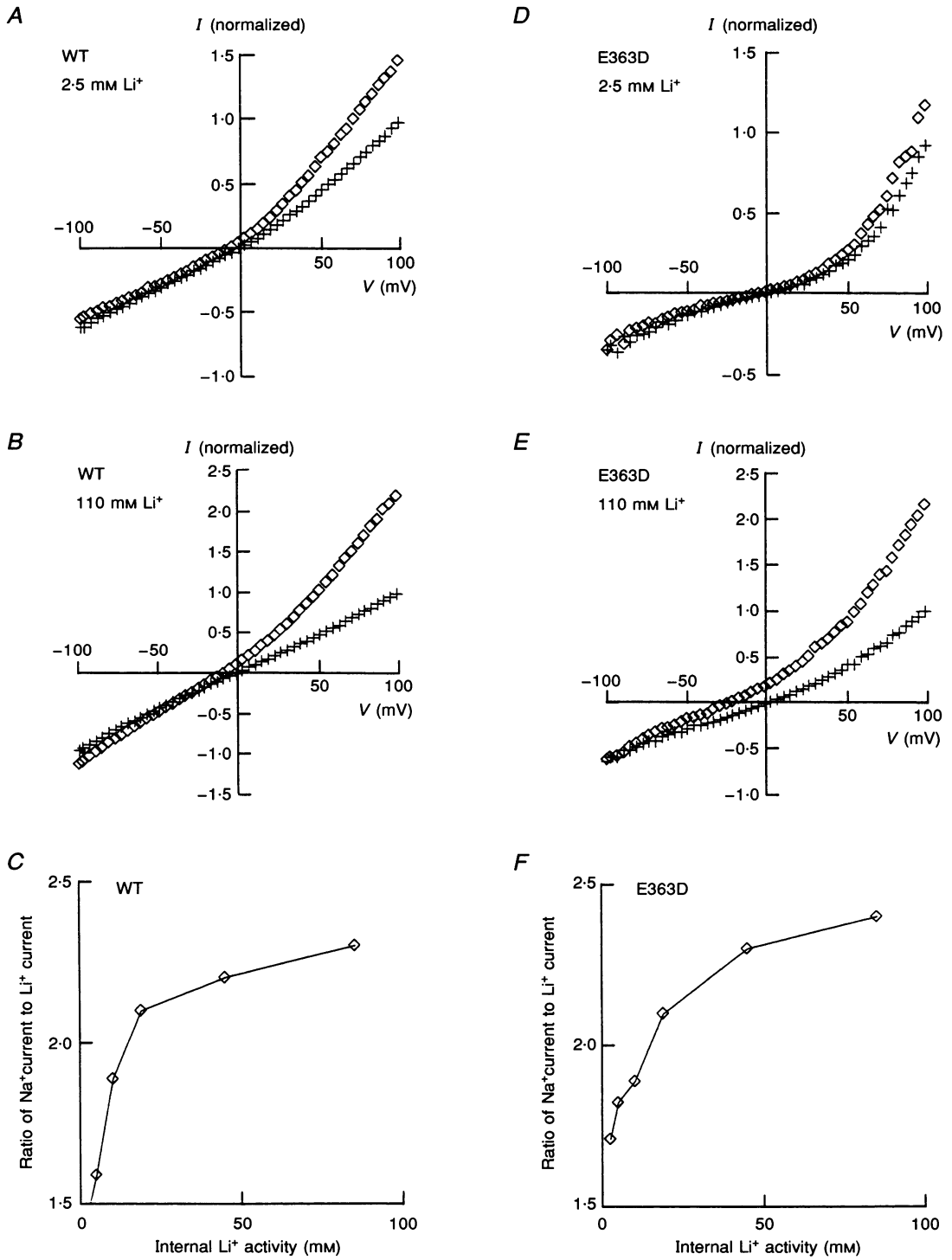

Figure 10. Determination of the low activity range for Li^+ in the WT and mutant channel E363D

In *A* and *D*, the patch pipette contained 2·5 mM Li^+ and the bathing medium an equimolar amount of Li^+ (+) or Na^+ (◇). In *B* and *E*, there was 110 mM Li^+ in the patch pipette. The current flowing in the presence of Li^+ in the bathing medium was 52, 250, 15 and 300 pA in *A*, *B*, *D* and *E*, respectively, and was normalized to 1. *C* and *F*, the relation between the ratio of the current flowing in the presence of Li^+ and Na^+ at +100 mV and the Li^+ activity inside the patch pipette for the WT and the mutant channel E363D, respectively.

channel E363D, respectively. As is the case for the native channel (see Fig. 4*D*), this ratio became close to 1 for ionic activities below 10 mM. All these experimental observations indicate that the WT channel and the mutant channel E363D, like the native channel, have a high affinity for Li^+ which decreases when the Li^+ activity is increased in the bathing medium, thus indicating that all these channels have a multi-ion pore.

The mutant channels E363Q and E363N are single-ion pores

As the mutant channels E363Q and E363N do not show any anomalous mole fraction effect and have permeability

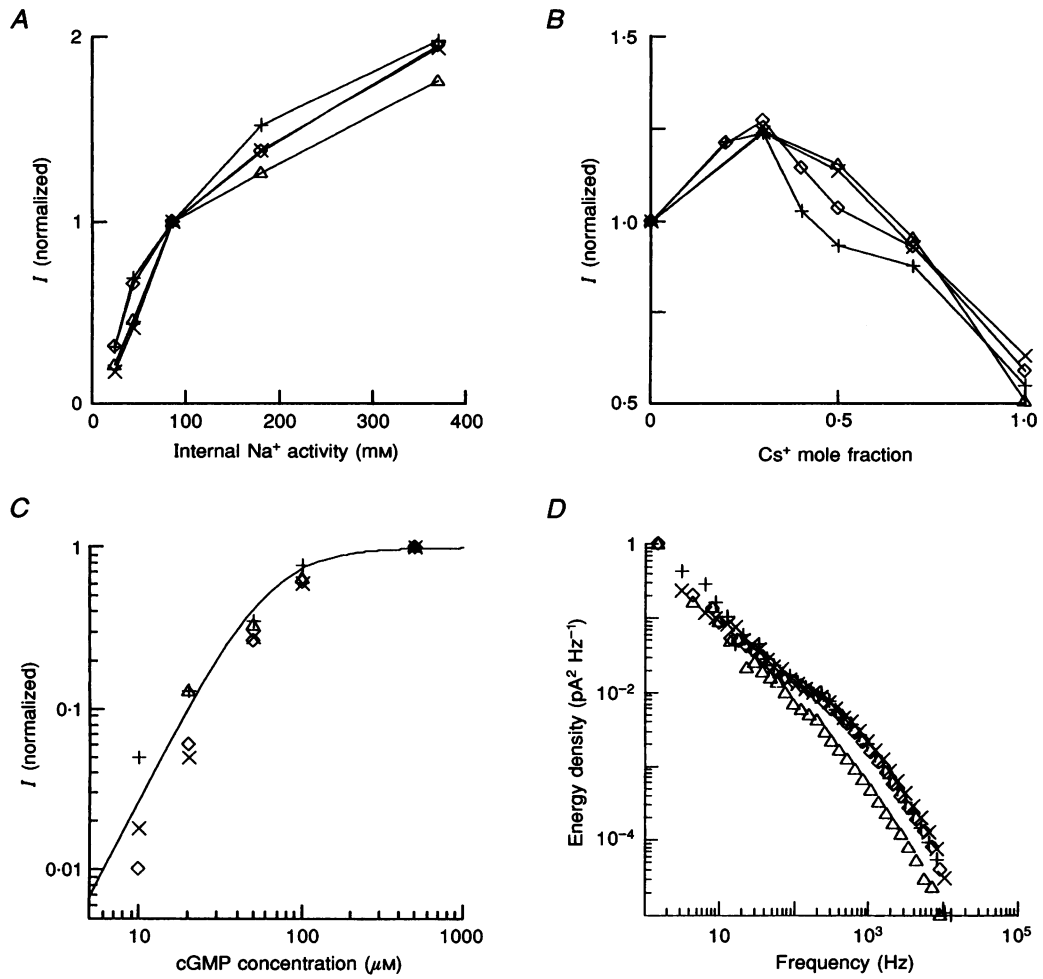

Figure 11. Electrical properties of mutant channels

A, the relation between outward current flowing at +90 mV and the Na^+ intracellular activity for the mutant channels K346Q (◇), R369Q (×), D370Q (△) and E372Q (+). The outward current was normalized to the current flowing at +90 mV in the presence of 110 mM Na^+. *B*, dependence of the outward current at +100 mV on the Cs^+ mole fraction in the bathing medium. Current was normalized to the current measured in the absence of Li^+. *C*, the relation between activated current and cGMP concentration in the bathing medium. Current normalized to the current flowing in the presence of 500 μM cGMP. The continuous line was obtained from the equation $I/I_{500} = [cGMP]^n/([cGMP]^n + K_m^n$, where I is the current activated by a given amount of cGMP, I_{500} is the current activated by 500 μM cGMP, [cGMP] is the cGMP concentration used to activate channels, K_m is the half-saturation cGMP concentration and n is a positive constant; the values for n and K_m were 2 and 60 μM, respectively. *D*, power spectra of current fluctuations at +100 mV induced by 500 μM cGMP. Power spectra were computed from current recordings filtered at 10 kHz with an 8-pole Butterworth filter and sampled at 30 kHz, with the exception of the power spectrum from the native channel, which was obtained from current recordings filtered at 20 kHz and sampled at 60 kHz. Each spectrum was obtained from current recordings of at least 10 s. Power spectra were obtained as the difference between the spectrum in the presence of cGMP and the spectrum in its absence. For a better comparison, individual power spectra were vertically scaled to have the same low-frequency asymptote as the mutant channel D370Q.

ratios very similar to conductance ratios (see also Eismann *et al.* 1994), it is interesting to verify whether the simple model of ionic permeation of Fig. 1 is consistent with the permeation of monovalent cations through these channels. Extensive analysis of the $I-V$ relations of the mutant channels E363Q and E363N, in a variety of experimental conditions, indicated that for ionic activities below 400 mM these channels behaved as single-ion pores with electrical distances equal for all ions and with the height of barriers B_1 and B_2 different for the various ions.

Neutralization of other charged residues in the putative pore region

The multi-ion nature of the cGMP-gated channel observed in the native and WT channel could originate from two different binding sites, or from the same binding site which can accommodate one or two ions at the same time, as proposed for Ca^{2+} channels (Armstrong & Neyton, 1991; Yang *et al.* 1993). In the case of two different binding sites within the pore, it is conceivable that the anomalous mole fraction effect could also be eliminated by the neutralization of other charged residues along the putative pore region. Consequently, aspartate and glutamate residues in positions 370 and 372 were mutated to a neutral glutamine. Similarly, lysine and arginine in positions 346 and 369 were neutralized and mutated to a glutamine.

All these mutations did not produce any major changes in the electrical properties of mutant channels. Figure 11 reproduces the results of different experiments with the mutant channels K346Q (◇), R369Q (×), D370Q (△) and E372Q (+). All these mutants exhibited a relation between the amplitude of the outward current (at +90 mV) carried by Na^+ or Li^+ and the internal ionic activity rather similar to that observed in the WT channel (see Fig. 11*A*). As shown in Fig. 11*B*, all these mutants exhibited an anomalous mole fraction effect with mixtures of Li^+ and Cs^+ almost identical to that observed in the WT channel (see Fig. 8*C* for comparison). Similarly, the relation between current amplitude and cGMP concentration in these mutants is almost identical to that measured in the WT channel (see Fig. 11*C*). The continuous line through the experimental points of Fig. 11*C* was obtained from the usual Hill equation (see figure legend) with the values 2 and 60 μM for n and K_m, respectively. These values are very similar to those obtained for the WT channel (Kaupp *et al.* 1989). No significant differences were observed in the shape of the power spectrum of current fluctuations at +100 mV induced by 500 μM cGMP (Fig. 11*D*). These results indicate that among the charged residues in the putative pore region, only glutamate 363 plays a significant role in ionic permeation.

DISCUSSION

In a previous analysis of the ionic permeation through the cGMP-gated channel, a simple model with a single binding site was able to reproduce successfully the shape of the $I-V$ relations under a variety of experimental conditions (Zimmerman & Baylor, 1992). Deviations from this simple behaviour were previously reported by Rispoli & Detwiler (1990) and Furman & Tanaka (1990).

This paper presents a variety of experimental results demonstrating that the cGMP-gated channel is a multi-ion pore and discusses the molecular basis of the multi-ion nature of the cGMP-gated channel.

Multiple occupancy

The good fit of the $I-V$ relations of Fig. 2*A* and *B* with eqn (4) and the independence of the reversal potential under bi-ionic conditions from the ionic concentration indicate that the ionic permeation of monovalent cations through the cGMP-gated channel can be described, in first approximation, by the simple model of Fig. 1*D*. The most striking deviations from the behaviour predicted by this model were observed when the permeation of Li^+ through the pore was analysed. When the Li^+ concentration was varied in the intracellular medium, the outward current carried by Li^+ both in the native and WT channel showed a moderate degree of saturation, suggesting a low affinity of the channel for Li^+ consistent with a well depth between 1 and $2RT$ (see Figs 2*B* and 3*D*). In contrast, some of the experiments described in Figs 3, 4 and 10, showing that the permeability ratio becomes similar to the conductance ratio for ionic activities below 5 mM, indicate a high affinity of the channel for Li^+ consistent with a much deeper well of at least $4RT$. The simplest way to explain this behaviour is to assume that the well depth for Li^+ decreases when the Li^+ concentration is raised on either side of the membrane. This behaviour can be explained by a binding site with an affinity modulated by the ionic strength of the medium bathing the intracellular face of the membrane, or by the simultaneous presence of at least two ions in the pore. In order to obtain evidence for the simultaneous presence of at least two ions within the pore, we have looked for an anomalous mole fraction effect between Li^+ and another ion. In agreement with previous reports, no anomalous behaviour with mixtures of 110 mM Li^+ and Na^+ was observed (Menini, 1990), but an anomalous mole fraction effect with mixtures of 110 mM Li^+ and Cs^+ was present (see Figs 5, 6 and 8). The observation of an anomalous mole fraction effect on the reversal potential of the WT channel indicates that the anomalous behaviour is not a consequence of an effect on the gating of a channel, but a genuine property of the channel.

The experimental observations reported in this paper indicate the simultaneous presence of at least two ions within the native and WT cGMP-gated channel and that multi-occupancy is the usual state of the channel. The proposed view of the inner core of the cGMP-gated channel is reminiscent of Ca^{2+} channels (Hess & Tsien, 1984; Almers & McCleskey, 1984; Kuo & Hess, 1993*a*, *b*; Kim *et al.* 1993; Yang *et al.* 1993; Eismann *et al.* 1994), where a

high-affinity binding site decreases its affinity as a consequence of a double occupancy of the channel.

The native and the WT channel

The properties of the macroscopic current flowing through the native cGMP-gated channel in tiger salamander rods and the WT channel (i.e. the α-subunit of the channel) from bovine rods are remarkably similar: both channels exhibit an anomalous mole fraction effect with Li^+–Cs^+ mixtures and the same transition between a high-affinity and a low-affinity binding site when the internal Li^+ activity is increased.

Molecular basis of the multi-ion behaviour of the cGMP-gated channel

As the amino acid sequence of the WT channel is known, it is possible to identify which amino acids contribute to the multi-ion nature of the pore. As shown in Fig. 1*A*, there are five charged residues in the putative pore region of the WT channel between lysine 346 and glutamate 372. Neutralization of the positively charged lysine 346 and arginine 369 and the negatively charged aspartate 370 and glutamate 372 did not modify major properties of ion permeation (see Fig. 11). The dependence of the outward current on the ion activity at the cytoplasmic side, and the anomalous mole fraction effect of the WT, was very similar to that of the mutant channels K346Q, R369Q, D370Q and E372Q. Only glutamate 363 appears to be crucial for the ionic permeation through cGMP-gated channels.

The outward current carried by monovalent alkali cations through the WT and the native channel (Menini, 1990; Zimmerman & Baylor, 1992) is half-saturated at an ion activity around 200 mM, whereas the mutant channels E363Q and E363N showed very little saturation even in the presence of ionic activities around 400 mM. The experiments reported in this paper indicate that the mutant channels E363Q and E363N are single-ion channels and have a very low affinity for monovalent cations, suggesting that the negative residue of glutamate 363 is the major binding site within the pore region. These results suggest that the co-ordination of several glutamates within the cGMP-activated channel provides the molecular structure able to bind one or two small cations, such as Li^+ or Na^+. These, and similar experiments performed on Ca^{2+} channels (Kim *et al.* 1993; Yang *et al.* 1993), reveal a striking similarity between cGMP-gated channels and Ca^{2+} channels, where the co-ordination of the negatively charged glutamates in repeat I–IV constitutes a binding site which can be occupied by one or two small ions and provides the molecular structure underlying the high turnover necessary for the physiological ionic permeation (Armstrong & Neyton, 1991).

Almers, W. & McCleskey, E. W. (1984). Non-selective conductance in calcium channels of frog muscle: calcium selectivity in a single-file pore. *Journal of Physiology* **353**, 585–608.

Armstrong, C. M. & Neyton, J. (1992). Ion permeation through calcium channels. *Annals of the New York Academy of Sciences* **635**, 18–25.

Baylor, D. A. & Nunn, B. (1986). Electrical properties of the light-sensitive conductance of salamander rods. *Journal of Physiology* **371**, 115–145.

Bönigk, W., Altenhofen, W., Müller, F., Dose, A., Illing, M., Molday, R. S. & Kaupp, U. B. (1993). Rod and cone photoreceptor cells express distinct genes for cGMP-gated channels. *Neuron* **10**, 865–877.

Bormann, J., Hamill, O. P. & Sakmann, B. (1987). Mechanism of anion permeation through channels gated by glycine and γ-aminobutyric acid in mouse cultured spinal neurones. *Journal of Physiology* **385**, 243–286.

Chen, T. Y., Peng, Y. W., Dhallan, R. S., Ahamed, B., Reed, R. R. & Yau, K. W. (1993). A new subunit of the cyclic nucleotide-gated cation channel in retinal rods. *Nature* **362**, 764–767.

Colamartino, G., Menini, A. & Torre, V. (1991). Blockage and permeation of divalent cations through the cyclic GMP-activated channel from tiger salamander retinal rods. *Journal of Physiology* **440**, 189–206.

Eismann, E., Müller, F., Heinemann, S. & Kaupp, U. B. (1994). A single negative charge within the pore region of a cGMP-gated channel controls rectification, Ca^{2+} blockage, and ionic selectivity. *Proceedings of the National Academy of Sciences of the USA* **91**, 1109–1113.

Furman, R. E. & Tanaka, J. C. (1990). Monovalent selectivity of the cyclic guanosine monophosphate-activated ion channel. *Journal of General Physiology* **96**, 57–82.

Gerasimov, Y. A. (1974). *Physical Chemistry.* MIR Publishers, Moscow.

Goulding, E. H., Tibbs, G. R., Liu, D. & Siegelbaum, S. A. (1993). Role of the H5 domain in determining pore diameter and ion permeation through cyclic nucleotide-gated channels. *Nature* **364**, 61–64.

Guy, H. R., Durell, S. R., Warmke, J., Drysdale, R. & Ganetzky, B. (1991). Similarities in amino acid sequences of *Drosophila eag* and cyclic nucleotide-gated channels. *Science* **254**, 730.

Hamill, O. P., Marty, A., Neher, E., Sakmann, B. & Sigworth, F. J. (1981). Improved patch-clamp techniques for high resolution current recording from cells and cell-free membrane patches. *Pflügers Archiv* **391**, 85–100.

Heginbotham, L., Abramson, T. & MacKinnon, R. (1992). A functional connection between the pores of distantly related ion channels as revealed by mutant K^+ channels. *Science* **258**, 1152–1155.

Herlitze, S. & Koenen, M. (1990). A general and rapid mutagenesis method using polymerase chain reaction. *Gene* **91**, 143–147.

Hess, P. & Tsien, R. W. (1984). Mechanism of ion permeation through calcium channels. *Nature* **309**, 453–456.

Hille, B. (1992). *Ionic Channels of Excitable Membranes.* Sinauer Associates, Sunderland, MA, USA.

Karpen, J. W., Zimmerman, A. L., Stryer, L. & Baylor, D. A. (1988). Gating kinetics of the cyclic GMP-activated channel of retinal rods: Flash photolysis and voltage-pump studies. *Proceedings of the National Academy of Sciences of the USA* **85**, 1287–1291.

KAUPP, U. B., NIIDOME, T., TANABE, T., TERADA, S., BÖNIGK, W., STÜHMER, W., COOK, N. J., KANGAWA, K., MATSUO, H., HIROSE, T., MIYATA, T. & NUMA, S. (1989). Primary structure and functional expression from complementary DNA of the rod photoreceptor cyclic GMP-gated channel. *Nature* **342**, 762–766.

KIM, M. S., MORII, T., SUN, L.-X., IMOTO, S. & MORI, Y. (1993). Structural determinants of ion selectivity in brain calcium channel. *FEBS Letters* **318**, 145–148.

KUO, C.-C. & HESS, P. (1993*a*). Ion permeation through the L-type Ca^{2+} channel in rat phaeochromocytoma cells: two sets of ion binding sites in the pore. *Journal of Physiology* **466**, 629–655.

KUO, C.-C. & HESS, P. (1993*b*). Characterization of the high-affinity Ca^{2+} binding sites in the L-type Ca^{2+} channel pore in rat phaeochromocytoma cells. *Journal of Physiology* **466**, 657–682.

LÜHRING, H., HANKE, W., SIMMOTEIT, R. & KAUPP, U. B. (1990). Cation selectivity of the cyclic GMP-gated channel of mammalian rod photoreceptors. In *Sensory Transduction*, ed. BORSELLINO, A., CERVETTO, L. & TORRE, V., pp. 169–174. Plenum Press, New York.

MELTON, D. A., KRIEG, P. A., REBAGLIATI, M. R., MANIATIS, T., ZINN, K. & GREEN, M. R. (1984). Efficient *in vitro* synthesis of biologically active RNA and RNA hybridization probes from plasmids containing a bacteriophage SP6 promoter. *Nucleic Acids Research* **12**, 7035–7056.

MENINI, A. (1990). Currents carried by monovalent cations through cyclic GMP-activated channels in excised patches from salamander rods. *Journal of Physiology* **424**, 167–185.

MENINI, A., RISPOLI, G. & TORRE, V. (1988). The ionic selectivity of the light-sensitive current in isolated rods of the tiger salamander. *Journal of Physiology* **402**, 279–300.

MILLER, J. I., PICONES, A. M. & KORENBROT, J. I. (1994). Differences in transduction between rod and cone photoreceptors: an exploration of the role of calcium homeostasis. *Current Opinion in Neurobiology* **4**, 488–495.

NIZZARI, M., SESTI, F., GIRAUDO, M. T., VIRGINIO, C., CATTANEO, A. & TORRE, V. (1993). Single channel properties of a cloned channel activated by cGMP. *Proceedings of the Royal Society* B **254**, 69–74.

PICCO, C. & MENINI, A. (1993). The permeability of the cGMP-activated channel to organic cations in retinal rods of the tiger salamander. *Journal of Physiology* **460**, 741–758.

RISPOLI, G. & DETWILER, P. B. (1990). Nucleoside triphosphates modulate the light-regulated channel in detached rod outer segments. *Biophysical Journal* **57**, 368A.

ROOT, M. J. & MACKINNON, R. (1993). Identification of an external divalent binding site in the pore of a cGMP-activated channel. *Neuron* **11**, 459–466.

SANGER, F., NICKLEN, S. & COULSON, A. R. (1977). DNA sequencing with chain-terminating inhibitors. *Proceedings of the National Academy of Sciences of the USA* **74**, 5463–5467.

SESTI, F., STRAFORINI, M., LAMB, T. D. & TORRE, V. (1994). Gating, selectivity and blockage of single channels activated by cyclic GMP in retinal rods of the tiger salamander. *Journal of Physiology* **474**, 203–222.

TORRE, V. & MENINI, A. (1994). Selectivity and single channel properties of the cGMP-activated channel in amphibian retinal rods. In *Handbook of Membrane Channels*, ed. PERACCHIA, C., pp. 345–358. Academic Press Inc., San Diego, CA, USA.

WEAST, R. C. (1986). *CRC Handbook of Chemistry and Physics*. CRC Press Inc., Boca Raton, FL, USA.

YANG, J., ELLINOR, P. T., SATHER, W. A., ZHANG, J.-F. & TSIEN, R. W. (1993). Molecular determinants of Ca^{2+} selectivity and ion permeation in L-type Ca^{2+} channels. *Nature* **366**, 158–162.

ZIMMERMAN, A. L. & BAYLOR, D. A. (1992). Cation interactions within the cyclic GMP-activated channel of retinal rods from the tiger salamander. *Journal of Physiology* **449**, 759–783.

Acknowledgements

We are indebted to Dr A. Menini for her critical reading of the manuscript. We appreciate the help of Miss M. Zanini who kindly typed the manuscript and Miss L. Giovanelli who did the artwork and checked the English. This research was supported by grants funded by the European Community (SSS 6961, Human Capital and Mobility Programme), by the Human Frontier Science Programme and by the Deutsche Forschungsgemeinschaft (U.B.K. and E.E.).

Received 6 October 1994; accepted 8 February 1995.